Accepted Manuscript

Title: Gold Laced Bio-macromolecules for Theranostic Application

Authors: Pranjali Yadav, Surya Prakash Singh, Aravind Kumar Rengan, Asifkhan Shanavas, Rohit Srivastava

Please cite this article as: Pranjali Yadav, Surya Prakash Singh, Aravind Kumar Rengan, Asifkhan Shanavas, Rohit Srivastava, Gold Laced Bio-macromolecules for Theranostic Application, International Journal of Biological Macromolecules https://doi.org/10.1016/j.ijbiomac.2017.10.124

Gold Laced Bio-macromolecules for Theranostic Application

Pranjali Yadav[1*], Surya Prakash Singh[2*], Aravind Kumar Rengan[2@], Asifkhan Shanavas[1@],
Rohit Srivastava[3@]

[1] Institute of Nano Science and Technology, Mohali, Punjab, India

[2] Department of Biomedical Engineering, Indian Institute of Technology Hyderabad, Telangana, India

[3] Department of Biosciences and Bioengineering, Indian Institute of Technology Bombay, Powai, Mumbai, India

[*]Equally contributing authors

[@]Correspondence:

asifkhan@inst.ac.in, akr@iith.ac.in and rsrivasta@iitb.ac.in

Abstract

Gold nanostructures are promising entities for various biomedical applications, due to their promising physical and optical properties. They can be tailored in different sizes and shapes to play vital roles for photothermal therapy, Biosensing, *In vivo* X-ray/CT contrast etc. Many biomacromolecules have been used for chemical reduction of ionic gold into zero-valent metallic nanoparticles of specific shape/size followed by stabilizing them for long term utilization. This review will sum up a range of biomacromolecules including Alginate, Agarose, Starch, Carragenan, Cellulose, Chitin, Chitosan, Collagen, Cyclodextrins, Chondrotin Sulfate, Dextran Sulfate, Fucoidan, Gelatin, Guar Gum and Hyaluronic Acid, whose functionalities have been explored in combination with gold nanoparticles for various biomedical applications.

1. Introduction

Nanotechnology is an interdisciplinary field that comprise of particulates and devices in nanometer scale, engineered with inputs from physics and chemistry. Application of nanotechnology in biomedical field is growing rapidly with advances in drug delivery, biomaterials and biosensing devices [1]. In need of constant improvement in the pharmacokinetics and therapeutic value of various drugs, nanotechnology has offered solution in the form of novel drug delivery systems [2]. Due to their enhanced physical, chemical and mechanical properties of nanomaterials compared to their bulk state, they have enormous potential in tissue regeneration. One of the major pathological condition that is addressed by nanomedical approaches is cancer. Currently cancer has become one of the leading causes of death worldwide. According to recent reports cancer is the second major cause of deaths in the world. It is reported by American Cancer Society that by 2030, 21.7 million new cases of cancer will be diagnosed globally [3]. Current strategies for the treatment of cancer depend on radiation therapy, chemotherapy, surgery photodynamic therapy, immunotherapy, hormonal therapy, vaccinations and stem cell transplantation. Among them, the conventional therapies can bear lot of side effects as well as there is possibility of development of resistance towards treatment [4-10]. In this framework, nanotechnology holds crucial role in drug delivery and imaging to specifically target cancerous cells without affecting healthy tissue. Nanoparticles have incredible physico-chemical properties as compared to their bulk counterparts because of high surface area to volume ratio. Nanoparticles show enhanced permeability and retention effect (EPR), where the nanoparticles gets delivered into tumor cells and stay in the tissue for longer time due to leaky tumor vasculature and poor lymphatic drainage respectively, making them suitable candidates for theranostic applications [11-14].

Among various types of inorganic nanomaterials, metallic nanoparticles such as gold nanoparticles (AuNPs) have been widely explored for therapy and imaging of cancer tissues. The AuNPs have been explored in many applications like biomedicine, photochemistry and electronics [15, 16]. The AuNPs have the ability for efficient conversion of light to heat and chief mediator of photothermal therapy (PTT) [17]. The AuNPs can be conjugated with ligands via gold-thiol bioconjugation for specific targeting to cancer cells. The AuNPs show better tumor penetration after systemic delivery due to the EPR effect [18-21]. Based on above mentioned

properties AuNPs mediated photothermal therapy (PTT) has been widely examined for tumor destruction in animal models and is presently in phase I human clinical trial studies [22-25].

The AuNPs have several distinguished properties that differentiate them from other nanomaterials. They can be synthesized with different shape **(Fig.1)** and size of ≥1 nm. The AuNPs are easily localized in abnormal cells and good carrier for drug loading [26, 27]. The significance of AuNPs in biomedical field is its promising physical and optical properties. When AuNPs are exposed to white light, the electrical component of the light polarizes the electrons present within the metallic nanocrystals forming a plasmonic dipole which oscillates in tune with the incoming light. When there is a frequency match between the plasma oscillation and that of the light, there is a significant absorption of energy at the corresponding wavelength of the light. This wavelength represents the Surface Plasmon Resonance (SPR) peak of a gold nanostructure. According to the SPR peak, the colloidal gold solution can appear blue, red, brown or green in color due to different shape and size of nanoparticle [28]. The extinction coefficients of gold nanoparticles are usually 4 to 5 times more than the conventional dyes [29]. As the SPR peak can be tuned to scatter light in Near Infra Red (NIR) region (700 to 1200 nm) of the spectrum, where there is minimal absorption of light by tissue components, anisotropic structures such as nanorods and nanoshells are extensively used for PTT and *in vivo* cancer diagnostic applications [30, 31]. Apart from size dependency of the SPR peak, simple aggregation of gold nanoparticles is known to red shift their plasmonic band [32]. Due to the anisotropic nature, AuNPs has tendency to form aggregates. Nature of the ligands as well as the high curvature causes the flocculation of AuNPs. Larger AuNPs generally form insoluble aggregates due to the inter particular interaction through weak hydrogen bonds, while small AuNPs covered with specific ligands have less chance of aggregation [33, 34].

Synthesis of stable AuNPs by decorating their surface with suitable bio macromolecules could improve the stability and avoid aggregation, making them appropriate for *in vivo* applications [35, 36]. Bio macromolecules exhibit excellent biodegradable and biocompatible characteristics. Using them for the reduction and stabilization of formed gold nanoparticles will not introduce any environmental toxicity or biological hazards. Several biomolecules such as chitosan [37-39], alginate [40], guar gum [41], fucoidan [42], starch [43], chitin [44], etc. have been used as reducing and stabilizing agent for the synthesis of GNPs. The most reliable and direct methods

available for the characterization of the GNP size, shape, and structure are UV-Vis spectroscopy, DLS, TEM and SEM electron microscopy.

While passive targeting of AuNPs by EPR effect is the most preferred approach, active targeting by surface modification can be achieved via conjugating specific ligands that binds to over-expressed membrane receptors on tumor cells. Ligands such as antibodies, peptides or oligosaccharides can improve tumor tissue targeting [45, 46]. Gold incorporated biomacromolecules can be used for theranostic applications as well as biosensors for cancer diagnosis. The AuNP-macromolecular composites have complementary functionalities for potential applications in the fields of photothermal therapy, wound dressing; SERS based biosensing and X-ray/Computer Tomography (CT) imaging **(Fig.1)**. This review will focus on a range of biomacromolecules including Alginate, Agarose, Starch, Carragenan, Cellulose, Chitin, Chitosan, Collagen, Cyclodextrins, Chondrotin Sulfate, Dextran Sulfate, Fucoidan, Gelatin, Guar Gum and Hyaluronic Acid, which are used in combination with AuNPs for various biomedical applications.

2. Gold-Biomacromolecule nanocomposites for biomedical applications

2.1 Chitosan-Gold Nanoparticles

Chitosan is a biopolymer derived from shrimp and crab shells. It is nontoxic, biodegradable, biocompatible and easy to process [47]. Chitosan acts as a protecting agent and can reduce gold salt to zero valent gold nanoparticles enabling green synthesis of AuNPs [37-39, 48-49]. Size of gold nanoparticles could also be tuned by using different molecular weight chitosan as reducing/stabilizing agent [50]. In addition, chitosan has also been used for NP coating and functionalization, to help anionic AuNPs acquire better stability in aqueous solution in comparison to uncoated AuNPs and display a positive surface charge to enhance NP cell uptake [51, 52]. The incorporation of chitosan during the synthesis of these metal nanoparticles offers better penetration and uptake of therapeutic agents. Devika *et al.* tested the enhanced penetration property, where CS coated on GNPs helps in the uptake of insulin by transient opening of the tight epithelial junctions. Different concentrations of chitosan were used for the synthesis of gold nanoparticles. At higher chitosan concentrations (>0.1% w/v) the gold NPs were stable (no

aggregation observed for 6 months). Loading efficiency of insulin was 53%. The blood glucose level was found to drop to 30.41 and 20.27% for oral (50 IU/kg) and nasal (10 IU/kg), respectively after two hours of administration. The serum gold levels for oral and nasal administration of chitosan reduced gold nanoparticles were found to be very low (0.053–0.072 ppm) as investigated by ICP measurements. These results established chitosan reduced gold nanoparticles as a promising delivery system for transmucosal application of drugs or peptides [53]. In another work, AuNPs encapsulated inside hollow hybrid structure of CS and polyacrylic acid (CS–PAA–Au hybrid) were prepared by a one pot aqueous synthesis route, for anti-cancer drug delivery. The CS–PAA–Au hybrid doped with cisplatin acted as a means of sustained drug delivery into the cells, as well as enters the nucleus and nucleolus. Due to large scattering cross section of gold NPs, these hybrid nanocomposites could be used as a contrast agent for dark field cell imaging [54].

A handful of reports have shown chitosan in conjunction with gold nanostructures in exploiting their exceptional photothermal efficiency for anti-cancer therapy. CS-gold nanorods hybrid nanocomposite particles have been reported to selectively target at the tumor site, to produce localized hyperthermia (temp. of 49 °C) after being exposed to NIR laser (808 nm). It was also found that the elevated temperature enhanced the efficacy of cisplatin, leading to multiple tumor suppression and complete tumor destruction [55]. Anisotropic heterogeneous gold nanostructures with controllable NIR absorption coated with CS, carboxy methyl chitosan and a mixture of both were synthesized and tested for their photothermal efficacy against HepG2 (Hepatocellular carcinoma) and HDF (Human dermal fibroblast) cells. The CS coated nanocomposite revealed the maximum photothermal efficiency on HepG2 cells [56]. Topete et al., reported the synthesis of polymeric gold nanohybrids by a seeded-growth method where chitosan acts as an electrostatic "glue" to attach Au seeds to DOXO/SPION-PLGA NP surface. Chitosan helps in the attachment of negatively charged gold seeds to the polymeric particle core and contributes as a weak reducing agent in the redox reaction of gold salt. Also, chitosan chains can act as a structure-directing agent supporting the growth of anisotropic gold shells. Gold seeds (4 nm) were deposited and further grown onto the surface of chitosan-modified DOXO-loaded PLGA NPs, further functionalized with a human serum albumin/indocyanine green/folic acid complex (HSA-ICG-FA) to configure a multifunctional nanotheranostic platform. The gold nanolayer was functionalized with an HSA-ICG-FA complex to provide, on one hand, stealth property to the

nanoplatform and, on the other, photodynamic therapy, fluorescence-based imaging, and active targeting properties [57, 58].

Besides being used as a photothermal agent or in photodynamic therapy, GNPs have been used as radiofrequency responsive nanomaterials for targeting various types of cancer [59]. Recently, Rejinold et al., synthesized curcumin loaded chitosan-graft-poly (N-vinyl caprolactam) nanoparticles containing gold nanoparticles (Au-CRC-TRC-NPs) by ionic cross-linking method. These NPs were used as an effective thermo-, pH- and RF-responsive curcumin delivery agent against tumor cells in vitro. In the presence of radiofrequency field the nano-curcumin showed controlled drug release, enhanced circulation and biodistribution than its bulk form of curcumin. The Au-CRC-TRC-NPs were retained in tumor for a week and 3.6μg/g curcumin was localized at the tumor. These NPs act as multi-responsive nanomedicine for RF-assisted cancer treatment modalities [60]. In another work, Au-CRC-TRC-NPs were used to selectively target breast cancer (4T1) cells. The haemocompatible Au-CRC-TRC-NPs were easily internalized by the breast cancer cells and essentially accumulated in the cytoplasm. The tumor localization studies demonstrate that Au-CRC-TRC-NPs could not only selectively accumulate at primary and secondary tumors but also show controlled drug release [61].

Chitosan-gold nanocomposites (colloids and films) were synthesized using three different chitosan grades varying in the molecular weight to obtain a material that is antimicrobial but non-cytotoxic. The nanocomposites were tested against *Staphylococcus aureus* and *Pseudomona aueroginosa*. The film based on chitosan with medium molecular weight (smallest average diameter ~ 15nm) showed the maximum antibacterial activity. AuNPs can interact with sulfur-containing proteins in the cell membrane changing its permeability, leading to leakage of intracellular components and finally cell death or/and bind to DNA and inhibit transcription [62]. However, when tested against mammalian cells (A549 and HaCaT) the same material did not show any cytotoxic behavior which makes them an ideal system for biomedical applications like wound dressing, adhesive bandages, coatings, etc [63]. Apart from possessing anti-bacterial and hemocompatible properties [64, 65], chitosan and its derivatives are also explored as hemostatic agents**.** Hemostatic chitosan nanocomposites were prepared from chitosan and gold nanoparticles (AuNPs) or silver nanoparticles (AgNPs) of ~5 nm size which showed greater elastic modulus, higher glass transition temperature and better cell proliferation than the pristine chitosan. Atomic force microscopy (AFM) demonstrated that the nanocrystalline domains on chitosan surface

were more evident upon addition of AuNPs or AgNPs (Fig. 4B). The potential of chitosan-Au nanocomposites as hemostatic wound dressings was evaluated in animal (rat) studies. Chitosan-Au was found to promote the repair of skin wound and hemostasis of severed hepatic portal vein. The effect of chitosan-Au on skin wound healing is shown in Fig. 4 C. Chitosan-Au promoted the rate of wound healing closure more than control (Tegaderm) and the original chitosan after surgery at 7 and 11 days, but not at 14 days (Fig. 4D). The histology at 7 days (Fig. 4E) showed the debris of chitosan (indicated by circles). In the hemostatic experiment, none of the original chitosan could stop the bleeding from hepatic portal vein when held on the wound. On the other hand, the dressings made from chitosan- Au stopped the bleeding effectively (n = 3) [66].

Chitosan modified AuNPs have been extensively used for sensing applications. An amperometric biosensor that measured plasma acetyl choline in healthy individuals and patients suffering from Alzheimer's disease has been developed. Acetyl choline (ACh) is a neurotransmitter found in PNS and CNS in all mammals including humans. During the course of the normal aging process, concentrations of ACh tend to decrease, resulting in the sporadic lapses of short-term memory in elderly individuals. A mixture of acetylcholinesterase and cholineoxidase (ChO) was immobilized onto a nanocomposite of Chitosan (CS)/gold-coated ferric oxide nanoparticles further electrodeposited on an Au electrode (acting as a working electrode). The sensor was used for the measurement of hydrogen peroxide formed by the oxidation of choline by immobilized ChO, produced from hydrolysis of acetyl choline. The sensor showed rapid response time (3s), low detection limit (0.005-400µM), good reproducibility and stability for 3 months (when stored at 4°C) [67]. Recently *Mycobacterium tuberculosis* (MTB) was taken as the model target for designing a nucleic acid detection platform using chitosan coated gold nanoparticles. The cationic AuNPs were used for the detection of specific MTB target amplified from total DNA extracted from sputum. It is a colorimetric sensor where the color of the solution changes from red to blue in case of positive samples, indicating a red shift in the plasmon resonance peak of gold. In contrast to this, the negative samples showed a blue shift. This assay was tested against 16 positive samples (15 were true positive) and 3 true negative samples. This is a cheap, simple and sensitive 1 tube-1 test colorimetric assay, which can be modified for the non invasive detection of other pathogens as well [68].

Chitosan based graphene-gold nanocomposite has been used for electrochemical detection of antigen associated with lung cancer. Here chitosan served as both reducing and stabilizing agent. These nanocomposites were used as electrochemical immunosensor to detect neuron-specific enolase (NSE). The results showed positive linear relationship for quantification of NSE with the concentration ranging from 0.1 to 2000 ng/mL. The lower limit of the detection was reported 0.05 ng/mL [69]. Chitosan oligosaccharide (COS) were used for AuNPs synthesis. COS was used as a reducing and stabilizing agent. These nanocomposites loaded with paclitaxel (PTX) were used in drug delivery and photoacoustic imaging (PAI). PTX loaded COS AuNPs showed pH-dependent drug release profiles. These nanocomposites showed significant cytotoxicity through enhanced reactive oxygen species (ROS) and induction of apoptosis. [70]. In another interesting work, a glucose sensor was developed by Zhang et al., (Fig. 2A) where the working electrode has a layer-by-layer (LBL) assembly of single-walled carbon nanotubes (SWNTs), multilayer films of chitosan (CS), gold nanoparticles (GNp), and glucose oxidase (GOx) for accurate detection of glucose levels in saliva. A working (sensor) electrode, a counter electrode, and a reference electrode were integrated on a single chip through micro-fabrication. This device is a simple, highly sensitive, accurate, convenient, low-cost, and disposable glucose biosensor on a single chip. The sensor features direct electron transfer between GOx and the electrode surface on-a-chip with LOD of 0.1 mg/dL i.e. 5.6 µM (Fig. 2B- 2D) [71].

Chitosan-modified popcorn-like Au–Ag nanoparticles (CSPNPs) based assay for high sensitive detection of melamine was developed by Li et al. in which CSPNPs not only possessed a higher intrinsic peroxidase activity but also acted as SERS substrates (Fig. 3A, 3B). CSPNPs can catalyze the oxidation of 3,3',5,5'-tetramethylbenzidine (TMB) by H_2O_2 to the charge transfer complex (CTC), which contributes to a tremendous surface-enhanced resonant Raman scattering (SERRS) signals with 632.8nm laser excitation. Melamine can generate an additional compound with H_2O_2, which means the available amount of H_2O_2 for the oxidation of TMB reduced. Hence, the SERRS intensity of CTC is decreased. The decreased Raman intensity is proportional to the concentration of melamine over a wide range (10nM-50µM) as shown in figure 3 (D), with a limit of detection (LOD) of 8.51nM. This highly selective method can be used for rapid, separation-free detection of melamine in milk powder [72].

2.2 Carrageenan-Gold Nanoparticles

Carrageenan is a high-molecular-weight, water-soluble sulfated polysaccharide extracted from red seaweeds. It has been extensively used as gelling agent in food and pharmaceutical industries due to their biocompatibility and ability to form thermoreversible hydrogels [73]. Carrageenan (CG) induced acute inflammation model compared with the effect of antioxidant N-acetylcysteine (NAC) alone and synergistic effect of AuNP along with NAC. The CG administered inflammation in pleural cavity causes increase the levels of myeloperoxidase, interleukin-1β, tumor necrosis factor-α and subsequently reduced the level of interleukin-10. Synergistic effects were observed after treatment of NAC and AuNPs resulting reduction of lipid peroxidation as well as oxidation of thiol groups [74]. In addition, thermo sensitive κ-carrageenan hydrogels in combination with spherical and rod-shaped AuNPs reported. The controlled drug release was observed from κ-carrageenan hydrogels. The release profile of drug was adjusted depending on morphology of AuNPs in κ-carrageenan hydrogels could be due to polymer relaxation mechanism or by diffusion. This kind of nanoformulation could be useful for enhancing AuNPs efficacy for cancer theranostics [75]. The conductive property of the Kappa Carrageenan-PolyPyrrole (KC-PPy) nano-composite has attributed to the successful fabrication of DNA biosensor. Esmaeili *et al.,* reported a DNA biosensor based on KC-PPy-gold nano-biocomposite for gender classification of Arowana fish. Thiol modified ssDNA probe sequence was immobilized on the surface of the composite via covalent attachment to the gold NP surface. The biosensor was selective (i.e. able to differentiate between complementary, non-complementary and mismatched bases), rapid (in terms of short assay time for DNA hybridization) and exhibited wider response range, lower limit of detection (LOD) and longer stability [76].

2.3 Alginate-Gold Nanoparticles

Alginates are naturally derived polysaccharides, composed of (1,4)-linked β-D-mannuronic acid (M-units) and R-L-guluronic acid (G-units) sugar residues [77]. Alginate is commonly considered to be a non-immunogenic polymer [78]. Coating GNPs with alginate-derived polymers provides them both colloidal stability and avoid recognition and sequestration by the body's defense system [79]. Alginate being a biopolymer, it was used as a reducing and

stabilizing agent for the green synthesis of AuNPs. The alginate stabilized AuNPs were loaded with two anticancer drug methotrexate and curcumin. This drug delivery system exhibited enhanced cytotoxic potential against C6 glioma and MCF-7 breast cancer cells apart from being hemocompatible. The structure of alginate being oxygen rich, it can effectively cap the AuNPs and protect them from aggregation [40]. Further, gold nanoparticles incorporated in alginate microcapsules (MCs) has been tested for the development of a micro-CT based tracking method. The gold labeled MCs exhibit bright contrast in rodent models, where due to high signal intensity, even reduced radiation dose is sufficient enough for tracking these particles. The post-mortem study data reveals that these particles can be used for longitudinal studies. Studies showed that high Hounsfield Units (HU) permitted appropriate visualization even when the image noise was high. HU signal range had the ability to distinguish between bone and soft tissue owing to contrast provide by AuNPs labeled MCs. It was confirmed that AuMCs could be observed even at lower concentrations of administered AuNPs as shown in Fig. 5 [80]. The developed imaging contrast agents have various advantages like ease of preparation, reduced cost of imaging technique and faster acquisition time. Instead of encapsulation, when the anionic alginate MCs are coated with cationic RAFT homopolymer modified AuNPs (PAuNPs) it resulted in hybrids which possessed low cytotoxicity and high mechanical stability in vitro. The localized gold concentration on the MCs exhibited a distinctive bright circular ring even with low X-ray dose and rapid scanning in post-mortem imaging experiments facilitating their positive identification and making them suitable candidate for in vivo tracking experiments in future [81]. An amperometric biosensor was developed by immobilizing gold nanoparticles-peroxidase nanosystem on alginate-coated gold electrode for the detection of hydrogen peroxide. Horseradish peroxidase was cross-linked with cysteamine-capped gold nanoparticles and immobilized on sodium alginate-coated Au electrode through polyelectrostatic interactions. The modified electrode showed fast electroanalytical response, good linear response and sensitivity, even at low concentrations of H_2O_2 [82].

2.4 Starch-Gold Nanoparticles

Starch, a glucose polymer, is one of the most abundant natural polysaccharides synthesized by plants. In its native state, starch is produced in granular form in plant cells mostly located in fruits, grains and roots/tubers [83, 84]. The use of natural starches as both the reducing and

stabilizing agents has become important in a green synthesis method of nanomaterials and nanocomposites [43]. The additional advantage of using starch is that there exists a specific enzyme to digest the polymer, which is useful for targeted delivery and appropriate use of the NPs at a desired site [85]. Gold Nps were synthesized by employing starch as both the reducing agent and the stabilizer. Starch modified AuNPs have been widely used for the sensing application. Pienpinijtham et al., produced starch-reduced gold nanoparticles and used it to determine the concentration of Iodide and Thiocyanate. Starch was degraded by alkali in order to enhance its reducing power. As a result, starch-reduced gold nanoparticles were obtained. These AuNPs were used to determine iodide and thiocyanate using SERS for the first time. Starch-reduced gold nanoparticles show an intrinsic raman peak at 2125 cm^{-1} due to the C=C stretching mode of a synthesized byproduct. Because of the high adsorptivity of iodide on a gold surface, the intensity of the SERS peak at 2125 cm^{-1} decrease with an increase in the iodide concentration. Thiocyanate also strongly adsorbs on a gold surface, and a new peak appears at around 2100 cm^{-1}, attributed to the C=N stretching vibration in a SERS spectrum of starch-reduced gold nanoparticles. These two peaks were successfully used to determine the iodide and thiocyanate concentrations simultaneously in a mixed sample. The detection limit of this technique for iodideis 0.01 μM with a measurement range of 0.01-2.0 μM, while the detection limit of this technique for thiocyanate is 0.05 μM with a measurement range of 0.05-50 μM. This technique is highly selective for iodide and thiocyanate ions without interference from other coexisting anions such as other halides, carbonate, and sulfate [86].

Engelbrekt et al., reported that the concentration of starch, temperature and chemical nature of the buffers play an important role in the AuNP formation. The synthesis has been tried with various starch rich vegetables (such as potato, carrot and onion). Boiling the fresh vegetables gives large amounts of starch and glucose, by hydrolysis. The most stable and reproducible procedure is achieved with potato extracts. The AuNPs efficiently enhance interfacial electrochemical electron transfer of the metalloprotein yeast cytochrome c in homogeneous solution, which is entirely absent on bulk Au (111) - or BPG electrode surfaces. Studies of the reaction of hybrids of AuNP with cyt C and AuNP with blue copper protein azurin, demonstrate the highly efficient, electronically rooted electrocatalytic properties of the AuNPs and size-dependent bioelectrocatalytic function of the AuNPs [87]. In another report, 20 nm starch-

stabilized gold nanoparticles were used for the development of an easy to use colorimetric assay for the detection of protein content in milk. The assay relies on the stabilization ability of proteins that inhibits the aggregation of AuNPs induced by hydrochloric acid. The degree of aggregation could be reduced in the presence of milk protein, depending on the total protein concentrations. As the total protein concentration decreases, the assay shows red to blue color shift. The assay is sensitive and can determine the protein content from 2.93×10^{-1} to 2.93×10^{-3} mg/mL via naked eye observation. The developed assay is very simple and requires 6 min for the whole analysis. This technique provides a great potential for on-site milk analysis, milk adulteration detection as well as in-house use [88]. T.K. Sarma et al reported starch mediated AuNPs synthesis having shape selectivity and tunable longitudinal plasmon band. The overall synthesis was carried out in presence of ultrasonic waves [89]. Z. Shervani et al reported formation of spherical NPs and nanowires of gold by using soluble starch and β-D-glucose. These monosaccharides (β-D-glucose) and polysaccharide (soluble starch) were used as stabilizing agents as well as structure directed synthesis of NPs [90].

2.5 Chitin-Gold Nanoparticles

Chitin is a sea food waste derived biopolymer that contains abundant hydroxyl and amino groups which makes chitin multifunctional such as [91, 92], reducing agent for AuNPs synthesis [44] and adsorbant for metal ions via chelation or ion exchange mechanisms [93-96]. In a recent work, deacetylated chitin nanofibrils acted as a reducing agent as well as stabilizer to immobilize the AuNPs due to the reducibility and chelation capacity of the amino groups on chitin. The positively charged AuNPs immobilized along the chitin nanofibrils possessed peroxidase-like activity and used for glucose detection via colorimetric method with a LOD of 94.5 nM. They catalyzed the oxidation reaction of 3, 3', 5, 5'-tetramethylbenzidine (TMB) by H_2O_2 to produce a blue solution [97]. In another report, gold based chitin–MnO_2 ternary composite nanogels (ACM-TNGs) were synthesized by the regeneration of chitin along with MnO_2 nanorods (5–20 nm) and the incorporation of Au-NPs. The ACM-TNGs showed cytocompatibility against various cell lines such as L929, HDF, MG63, T47D and A375 without affecting the cellular morphology. ACM-TNGs were successful in killing breast cancer cells under RF radiation at 100 W for 2 min. The ACM-TNGs exhibited applied power dependent RF heating, which could be useful for magnetic hyperthermia for cancer therapy [98].

2.6 Cellulose-Gold Nanoparticles

Cellulose is a fibrous, tough, water-insoluble substance, which is found in the protective cell walls of plants, particularly in stalks, stems, trunks and all woody portions of plant tissues. An unbranched homopolysaccharide, cellulose is composed of β-D-glucopyranose units linked by (1-4) glycosidic bonds [99, 100]. Bacterial Cellulose (BC) has gained more interest in commercial applications in the past few years in various industries (paper, headphone membranes, food and textiles) and biomaterials including temporary skin substitute, artificial blood vessels, and nerves [101-103]. Biocompatible cellulose nanocrystal (CNC) was used as substrate for loading spherical gold nanoparticles (AuNPs) or gold nanorods (Au NRs). AuNPs or AuNRs conjugated with CNC through gold-thiolate bonds, formed hetero-layered nanohybrids and was used for effective cancer therapy. As showed in Fig. 6A, CNC-Au nanohybrids were conjugated to CD-PGEA (comprising β-cyclodextrin cores and ethanolamine-functionalized poly (glycidyl methacrylate) arms) via gold-thiolate bonds and host-guest interaction. TEM images of CNC-Au NR revealed the successful fabrication of AuNPs/AuNRs on the surface of CNCs. CNC-Au-PGEA nanoparticles have efficient transfection abilities. The enhanced fluorescence of green fluorescent protein (EGFP) in C6 cells due to gene expression of plasmid pEGFP-N1 has been shown (Fig. 6B, 6C). The AuNRs and CNC-Au NR-PGEA2 showed peak at ~800 nm due to strong longitudinal surface plasmon resonance. The temperature increment for CNC-Au NR-PGEA2 by 808 nm laser irradiation under aqueous condition was observed by thermal imaging camera. Histology analysis of the tumor cells showed clear necrosis, nuclear fragmentation and massive karyopyknosis after treatment confirming the promising photothermal enactment of CNC-Au NR-PGEA2. Beside this, CNC-Au NR-PGEA2 has also been projected as ideal contrast agent for photoacoustic imaging as shown in Fig. 6D (a-j). These nanohybrids were used for combined photothermal/gene therapy as well as photoacoustic imaging [104]. Gold-cellulose nanocomposite has been used to immobilize heme proteins such as horseradish peroxidase (HRP), hemoglobin (Hb) and myoglobin (Mb) on the surface of modified glassy carbon electrode (GCE). Results showed that the gold–cellulose nanocomposite promotes the electron transfer, accelerates the mass transport and enhances the mechanical stability of the immobilization. HRP immobilized in the gold-cellulose film showed the highest biocatalytic activity with good sensitivity, low detection limit and fast response

toward hydrogen peroxide detection. The HRP based sensor exhibited a fast amperometric response (within 1 s) to H_2O_2, a good linear response over a wide range of concentration from 0.3mM to 1.00mM, and a low detection limit of 0.1 µM [105].

2.7 Collagen-Gold Nanoparticles

Collagen is the most abundant protein in the animal body and is the predominant protein for bone biomineralization and promotes the enhancement of the mechanical property of the extracellular matrix [106, 107]. A combination of collagen and mineralized inorganic nanoparticles (such as AuNPs) are particularly advantageous for application in tissue engineering, regenerative medicine, and drug delivery owing to their excellent biocompatibility, moderate immunogenicity, and enhanced mechanical properties [108, 109]. Collagen such as type I collagen contains a number of hydroxyproline residues capable of donating electrons [110, 111] and could thus be suitable for reduction of gold salts. Collagen scaffolds incorporating gold nanoparticles (AuNPs) were prepared and used for wound healing applications. The collagen/gold nanoparticles nanocomposite acted as a potential skin wound healing biomaterial and was investigated for in vitro biocompatibility and in vivo effects such as induction or inhibition of inflammatory responses influence on the wound closure and possible contribution to the enhancement of re-epithelialization, neovascularization and granulation tissue formation [112, 113]. The AuNPs with size (>20 nm) and dose (<20ppm) were not cytotoxic on HaCat keratinocytes and 3T3 fibroblasts, hence they were incorporated into collagen scaffolds. These nanocomposites showed improvement on properties of collagen scaffolds as higher resistance against hydrolytic and enzymatic degradation, and higher tensile strengths. In vivo studies revealed promising healing effects of crosslinked collagen/gold nanoparticle nanocomposites, improved TS and elastic modulus, high-wound closure percentage, reduced inflammatory response, increased neovascularization, and granulation tissue formation than any other treatment group (CS-X and/or Matriderm) or untreated control group. The overall effect of AuNPs can be enhanced by increasing the concentration of AuNPs [114].

2.8 Agarose-Gold Nanoparticles

Agarose is a straight-chain polysaccharide extracted from seaweed or other vegetables. Agarose powder is soluble in water when heated above 90°C. When cooled down to room temperature (25–35 °C) it forms a semi-solid gel. The gel gelation characteristics created by the presence of hydrogen bonds can be destroyed by any factor lead to the destruction of hydrogen bonds. The pore size of agarose could be changed by the concentration of agarose powder. The gelling properties, stability, shrink and swell features; absorption behavior has made agarose gel more accessible in the food, pharmaceutical, chemical and textile industries [115-117].

Agarose-stabilized gold nanoparticles yield higher SERS activity for DNA nucleosides which gives the freedom of using this AuNP for on-chip biosensing applications. The SERS activity of nucleosides with Agarose-AuNP was compared to that of commercially obtained citrate-stabilized gold nanoparticles and the results reveal that the SERS signals obtained with Agarose-AuNP was found to be more as compared to the other one. The higher SERS activity is explained in terms of the agarose matrix, which provides pathways for the gold nanoparticles to have distinct arrangements that result in stronger internal plasmon resonances. The work reported that the agarose stabilized AuNPs can detect DNA nucleosides in micromolar range by using SERS. The SERS activity of nucleosides with agarose AuNPs was more pronounced as compared to that of commercially obtained citrate-stabilized AuNPs. Agarose stabilized AuNPs guarantees nondegradation of probe molecules. On the other hand, the gelation property of agarose can enable easy film formation that could be useful for on-chip biosensing applications [118]. AuNPs improve the SERS activity which can be helpful for on-chip biosensing applications towards detection of single molecules as well as identifying their chemical structure. SERS now offers label-free detection of biomolecules. Binding of oligonucleosides to AuNPs surface can enable to detect multiplexed DNA. The real-time DNA detection methodology can be done via rapid sequencing of single DNA bases due to SERS properties of AuNPs [119]. Agarose gel was used as a template for the preparation of gold nanoparticles–agarose gel composite by adsorption of prepared colloidal GNPs. The shrink–swell properties of agarose gel combined with the optical absorption properties of GNPs, make the composite film an eligible SERS substrate for the detection of Raman signal for various molecules (such as Niel blue A sulfate (NBA), 4-mercaptobenzoic acid (MBA), 1-naphthalenethiol (1NAT)). When the composite film was

exposed to the air, the agarose gel started to dehydrate and eventually shrinked. The GNPs got close to each other and the hot-spot effect generated. Results revealed that this composite film could be used as an effective SERS substrate for the detection of Raman signal molecules (NBA, MBA, 1NAT). The SERS signal showed a gradual increase upon the dehydration process due to the dynamic hot-spot effect. Raman molecules can be washed by a cleaning solution and reused [120].

2.9 Chondroitin sulfate-gold nanoparticles

Chondroitin sulfate (CS) is a sulfated glycosaminoglycan (GAG) that is composed of two monosaccharides arranged alternatively with D-glucuronic acid (GlcA) and N-acetyl-D-galactosamine (GalNAc). These two monosaccharides of chondroitin made up of 100 individual sugars that can be sulfated at distinct positions. These sulfated chondroitin attach with protein in the form of a proteoglycan. CS is one of the most important structural constituents of cartilage [121]. Chondroitin is also used as a therapeutic moiety to treat osteoarthritis and approved as a symptomatic slow-acting drug [122, 123]. Liu et al., reported a new switch-off fluorescent probe using CS for uric acid determination based on the inner filter effect (IFE). As the IFE absorber/fluorophore had poly (vinylpyrrolidone)-protected gold nanoparticles (PVP-AuNPs) and chondroitin sulfate-stabilized gold nanoclusters (CS-AuNCs). The detection limit was around 0.3μM [124]. Gurav D et al, reported chondroitin sulfate (CS) coated gold nanoparticles as a novel approach to resolve multidrug resistance and thrombo inflammation triggered by the chemotherapeutic drug [125]. According to Ma et al, quantitative analysis of CS is possible with interaction among CS and AuNPs and silver nanoparticles (SNPs) by observed spectral changes in absorbance. Surface Plasmon Resonance (SPR) was used to examine the characteristics of their spectrum after interaction. The method was useful for the determination of the CS contents from different biological origins. The results showed that there are no such effects by small quantity of blood plasma on the determination of CS even when the CS to heparin concentration ratio was more than 10:1 [126]. In another work, AuNPs were used as drug delivery vehicle for enhancing the delivery of CS and exhibited the potential of AuNPs-CS for the treatment of osteoarthritis. AuNPs-CS was known to stimulate cell proliferation and cause the two-fold increase in glycosaminoglycan and collagen production when compared to native CS [127]. According to report of Cho HJ et al synthesized CS capped AuNPs and were used them for

delivery of oral insulin (INS) under *in vivo* condition was investigated. CS-capped AuNPs when loaded with INS with about 123 nm mean diameter and they were found to stabile for upto 7 weeks. It was observed that AuNPs/INS showed 6.61 fold higher INS concentration in blood plasma level after 120 min of oral administration in streptozotocin induced diabetic rat model as compared control group [128]. Noh HJ et al reported that CS-reduced AuNPs can be a promising method for rapid on-site melamine screening in milk products. Here AuNPs were green-synthesized by interaction of Au^{3+} and CS raising temperature. The yield ratio of Au^{3+} to Au^0 after CS induced reduction of gold was 80.1%. CS reduced AuNPs were used as nanosensor to detect melamine. It showed linear relationship with absorbance ratio (A620nm/A530nm) with melamine concentration range between the 0.1-10 µM. The lowest detection limit of melamine quantified was lower as 12.6 ppb [129]. Kalita M et al reported a ultrasensitive technique of sensing oversulfated chondroitin sulfate (OSCS) in heparin by means of a nanometal surface energy transfer (NSET) that was based on gold heparin dye nanosensor. This was able to detect OSCS with concentration as low as 1×10^{-9} % (w/w) that can be useful for validation of pharmaceutical heparin [130].

2.10 Gelatin-gold nanoparticles

Gelatin is usually derived from animal tissues including bones and skin of animals such as domesticated cattle, pigs, chicken and fish. Gelatin is a kind of mixture made up of protein and peptides after partial hydrolysis of collagen derived from animal body tissue. It is virtually tasteless and colorless [131]. Suarasan et al reported FLT3 inhibitors via gelatin-coated gold nanoparticles for the treatment of acute myeloid leukemia with better efficiency. FLT3 inhibitors, namely midostaurin, sorafenib, lestaurtinib, and quizartinib were individually loaded onto gelatin-coated gold nanoparticles. Among them quizartinib-loaded AuNPs were investigated against OCI-AML3 acute myeloid leukemia cells and were shown to improve drug's efficacy [132].

2.11 Fucoidan-gold nanoparticles

Fucoidan is a sulfated polysaccharide (molecular weight: average 20,000) found in various species of brown seaweed/algae. Fucoidan (Fu) is one of the important ingredient in dietary

supplement products. It is a group of fucose containing sulfated polysaccharides with backbone made up of (1→3)-linked α-l-fucopyranosyl or of alternating (1→3)- and (1→4)-linked α-l-fucopyranosyl residues. These sulfated polysaccharides have potentially useful bioactive functions for humans [133]. It is a naturally occurring polysaccharide component that is also having anti-cancer activity. It can target key apoptotic molecules involved in cancer progression. It can selectively harm cancer celland overcome the systemic toxicity to healthy cells during chemotherapy and radiation therapy. Thus Fucoidan can be used to show significant synergistic effect with other anti-cancer agents [134]. Fucoidan displays anti-cancer property by various mechanisms such as induction of apoptosis, cell cycle arrest and immune system activation. In addition to this, fucoidan can also induce inflammation through immune system, stem cell mobilization and oxidative stress as reported by Kwak et al [135]. Manivasagan P et al demonstrated that biocompatible AuNPs were synthesized by means of a naturally occurring fucoidan and was used as both capping as well as reducing agent. Fu-AuNPs loaded with doxorubicin (DOX) can be used for drug delivery and photoacoustic imaging (PAI). The release kinetics shows that the release of DOX from DOX-Fu AuNPs was greater in acidic pH (4.5) as compared to physiological pH (7.4). Cytotoxic efficacy of DOX-Fu AuNPs (inhibitory concentration of 5μg/ml) at 24h can inhibit the proliferation of human breast cancer cells. The DOX-Fu AuNPs could also be used for photoacoustic imaging (PAI) of breast cancer cells [42]. In another report, AuNPs coated with fucoidan-mimetic glycopolymers exhibited promising anti-cancer properties. They showed selective cytotoxicity to human colon cancer cell lines (HCT116), with significant biocompatibility to mouse fibroblast cells (NIH3T3) [136].

2.12 Guar gum-gold nanoparticles

Guar gum (guaran) synthesized from guar beans which has stabilizing as well as thickening properties [137]. Pandey et al, reported a cost effective and eco-friendly method for the synthesis of AuNPs using guar gum (GG) as a reducing agent. GG/AuNPs nanocomposite was used for detection of aqueous ammonia based on SPR and detection limit of ammonia was around 1ppb (parts-per-billion) [41].

2.13 Hyaluronic acid-gold nanoparticles

Hyaluronicacid (HA), a naturally occurring polysaccharide composed of N-acetyl-d-glucosamine and d-glucuronic acid arrange alternatively. HA have strong affinity with CD44cell-specific surface marker, which is overexpressed in many cancer cell types. It plays an important role in cell migration under compact tissue environment by offering an open hydrated matrix that enables cell migration. [138]. It is known to have specific interaction between HA and cell surface HA receptors, RHAMM (receptor for hyaluronan-mediated motility), HARE (HA receptor for endocytosis) facilitate cell migration [139-142]. Short oligomers of HA are known to possess (3–9 disaccharide units), shows anti carcinogenic effect [143, 144].

Hosseinzadeh H. et al reported, SN38conjugated to negatively charged HA, further deposited over positively charged AuNPs through electrostatic interaction. Under in vitro condition drug release was increased up to 30 % in acidic conditions (pH 5.2) after red LED illumination (6min) as compared to control. The combination therapy was found to have reduced the migratory potential and increased the toxicity against HT29, SW480 and CHO cells [145]. For tumor diagnosis and therapy multifunctional nanoprobes are drawing more attention. Li B et al reported two types of nanoprobes viz gold nanorods and gold nanospheres. These AuNPs were coated with thiolated-hyaluronic acid labeled with nile blue, which enhanced cellular uptakes in human breast carcinoma cells (MCF-7) through overexpressedCD44 receptor. Studies suggested that rod-shaped bioprobe were outstanding candidates for imaging and photothermal therapy to MCF-7 cells [146]. According to Kumar et al, HA served as a capping as well as targeting agent for metformin delivery with AuNPs. Evaluation of synthesized HA-AuNPs loaded with metformin showed significant reduction in G2/M phase of HepG2 cells and reduced their growth as compared to free metformin [147]. Zhao L et al reported SERS active gold nanochains (AuNCs) were used for detection and photodynamic therapy (PDT) of cancer. AuNCs were prepared by using HA as a template. AuNCs have an effective SERS property and exhibited maximal absorption at near-infrared (NIR) region. These nanoformulations showed better cellular uptake with excellent phototoxicity [148]. Lin CM et al, reported that Benzo[a]pyrene (BaP) (present in cooking oil fumes) can stimulate lung cancer cell proliferation due to the induction of inhibitor of apoptosis protein-2 (IAP-2). They synthesized a biocompatible HA coated AuNPs loaded with IAP-2-specific small-interfering RNA (siRNAs). AuNP-HA were

taken up effectively byA549 cells through CD44-mediated endocytosis. Cell migration and matrix metalloproteinase-2 were suppressed after treatment with AuNP-HA-IAP-2 siRNAs [149]. Li J et al reported use of HA-modified Fe3O4@Au core/shell nanostars (Fe3O4@Au-HA NSs) for computed tomography (CT), magnetic resonance (MR) and photothermal therapy of cancer were explored. Synthesized Fe3O4@Au-HA NSs NIR having absorption properties that allows nanoprobe for imaging and photothermal ablation of cancer cells under both in vitro and in vivo conditions [150]. Song Y et al reported, AuNPs were functionalized with HA, cresyl violet and porphyrin to be used as nanoprobe. They were used for phototherapy and fluorescence imaging via enhanced cellular uptake.Here the nanoprobe became highly fluorescent under ultraviolet irradiation and in the presence of hyaluronidase enzyme [151]. Li N et al reported a biocompatible nanoformulation of cyclodextrin-grafted hyaluronic acid constructed from AuNPs (HACD-AuNPs) for the delivery of drugs such as doxorubicin hydrochloride (DOX), camptothecin, irinotecan hydrochloride, paclitaxel and topotecan hydrochloride. Toxicity of Dox was minimized with aid of nanoformulation (HACD-AuNPs) [152].

2.14 Cyclodextrin-gold nanoparticles

Cyclodextrins are made up of sugar molecule produced after enzymatic conversion of starch. It is used for drug delivery and pharmaceutical applications [153, 154]. Cyclodextrin is made up of 5 or more α-D-glucopyranoside units. They have varying number of glucose monomer and are categorize depending on glucose monomer ranging from six to eight units present in a ring. Types of cyclodextrin include, α (alpha) cyclodextrin (6-membered sugar ring molecule), β (beta) cyclodextrin (7-membered sugar ring molecule) and γ (gamma) cyclodextrin (8-membered sugar ring molecule) [155]. Hu Yet al, reported a biocompatible cellulose nanocrystal (CNC)-AuNPs hybrid with rod-like morphology. This hybrid contains β-cyclodextrin cores and ethanolamine functionalized poly (glycidyl methacrylate) arms through gold thiolate bonds with host-guest interaction. This nanohybrid was used for photoacoustic imaging and combined photothermal/gene therapy of cancer [156]. Lee D et al, reported AuNPs conjugated with thiolated beta cyclodextrin (AuNP-S-β-CD) loaded with Baicalin, an anti-cancer drug can induce apoptosis in MCF-7 cells. Western blot analysis revealed that the cell death happening via induction of apoptosis in MCF-7 cells [157]. Chen W H et al, reported a multifunctional nanocomposite based on AuNP@CD with pH sensitive anticancer prodrug AD-Hyd-DOX and

cancer-targeted peptide AD-PEG8-GRGDS. Nanoparticles were constructed by host-guest interaction for active targeting of cancer. AuNP@CD-AD-DOX/RGD nanocomposite showed selective uptake in cancer cells due to receptor-mediated endocytosis. They showed triggered release in acidic environment and induced apoptotic cell death in cancer cells [158]. Bakar *et al* reported, three lignan conjugated AuNPs were synthesized. Surface modification of AuNPs performed by using thiolated β-cyclodextrin (β-CD) for imaging as well as for drug delivery applications. They investigated the antiproliferative properties of three lignans-AuNP conjugates, lariciresinol, pinoresinol and secoisolariciresinol on the MCF-7 cell lines [159]. Mieszawska AJ et al reported, poly(lactic-co-glycolic) acid (PLGA) polymer-lipid NP loaded with doxorubicin in polymeric core and sorafenib (anti-angiogenic drug) loaded in lipid corona. The nanoformulation made of cyclodextrin which contained doxorubicin encapsulation in the core of nanoparticles and gold nanocrystals for imaging. Release kinetics of nanoparticles showed rapid release of the sorafenib (corona drug) and late release of doxorubicin (core drug) [160]. According to another report by Heo DN et al, AuNPs with rhodamine B linked beta-cyclodextrin (β-CD) was used for therapy as well as diagnosis of the cancer cells. AuNPs surface-functionalized with PEG, paclitaxel (PTX) and biotin can be beneficial for cancer therapy as a theranostic agent without any systemic toxicity to normal cells. PTX (anti-cancer agent) was effectively released from nanoformulation using the intracellular glutathione (GSH, 10 mm) [161].

2.15 Dextran sulfate-gold nanoparticle

Dextran is made up of glucose molecules arranged in complex branched glucan (polysaccharide) having varying chain length ranging from 3 to 2000 kilo Daltons. Glucose molecules are linked together via α-1, 6 glycosidic linkages, while α-1,3 linkages formed between branches. On the other hand, dextran sulfate comprises approximately 16–19% sulfur that is corresponding to almost 1.6–2.4 sulfate groups per glucosyl unit [162]. Dextran sulfate is biocompatible as well as biodegradable anionic biopolymer [163]. Saksono B et al, reported new technique with the aid of identifying trace amounts of dengue virus (DENVs) from serum sample. In this method sulfated sugar chain-immobilized over the AuNPs interacts with DENV's surface glycoprotein resulting in precipitation of the complex. Reverse-transcription quantitative polymerase chain reaction used to detect the viral RNA content. These nano formulations have greatest sensitivity; detect low concentrations of DENVs

by using only 6 μL of serum sample [164]. In another report, AuNPs was shown to detect DNA mismatches and damages by using oligonucleotide-modified AuNPs as a probe. The hybridization of AuNP probes and target DNA results in nanoparticle aggregation. Further addition of dextran sulfate can separate out non-aggregated AuNPs from aggregated ones causing change in the absorption band [165].

3. Conclusion & Future Perspectives

Table-1 summarizes various AuNP-Biomacromolecule nancomposites for therapy and diagnostic applications. AuNPs have promising approach for drug delivery, imaging and cancer treatment. Wide varieties of biological macromolecules are used in combination (surface modification [146, 166, 167], direct covalent conjugation [149, 151, 158, 168], ionic interaction [71, 80, 136] etc) with AuNPs. These modifications are helpful for combinatorial therapy by incorporating chemotherapeutic drugs. Reports have shown that biopolymers in combination with gold nanostructures are excellent candidates for active targeting, bio sensing and sustained drug delivery applications. Several kinds of nanoformulation based on AuNPs are being prepared by synthetic methods and deployed in pre-clinical studies. Biomacromolecule - AuNPs mediated photothermal effect can be augmented with increased tumor accumulation of nanoformulations. The extinction coefficients of AuNPs are higher as compared to dyes, leading to promising platform for imaging as well as sensing of trace elements. Green-synthetic methods are applied to make biocompatible AuNPs in combination with biological macromolecules that can improve therapeutic effects by enhancing cellular uptake at tumor site. Synergistic effects are observed when PTT and chemotherapeutic drugs are combined with biological macromolecules. These multifunctional nanosystems shall impart effective and specific cancer cell killing by avoiding the systemic toxicity to normal cells thereby playing an important role in translational cancer research.

While more research work is required for few biomacromolecules such as carrageenan, gelatin and guar gum in combination with AuNPs, the existing pool of knowledge provides fair insight into the potential of all the composites discussed for various biomedical applications, especially biosensors. As most of the macromolecules discussed in this review are water soluble and biocompatible, wearable and washable sensors from some of these nanocomposites for

measuring analytes in sweat have huge potential for translation. Such wearable devices could also be extended as dressings, where AuNPs can detect presence of any infection over the course of wound healing. Post surgical implants of these nanocomposites for photothermal treatment of residual tumours can also be explored. Even though gold-biopolymer composites are so far tested only up to preclinical stage, the clinical trials of gold based nanomaterials [169] and few of the biopolymers such as Dextran [170] and β-cyclodextrin [171] provides a positive outlook on the translational potential of their composite structures.

Acknowledgements

References:

[1] Nanotechnology in Therapeutics: Current Technology and Applications, in: Nicholas A. Peppas, J. Zach Hilt, J. Brock Thomas (Eds.), Horizon Bioscience, 2013.

[2] Suwussa Bamrungsap, Zilong Zhao, Tao Chen, Lin Wang, Chummei Li, Ting Fu & Weihong Tan, Nanotechnology in therapeutics: a focus on nanoparticles as a drug delivery system, Nanomedicine, 7 (2012), 1253–1271.

[3] American Cancer Society, (2015) http: // www.cancer.org /acs/ groups/content /@research / documents/document/acspc-044738.pdf.

[4] C.R. Patra, R. Bhattacharya, D. Mukhopadhyay, P. Mukherjee, Fabrication of gold nanoparticles for targeted therapy in pancreatic cancer, J Biomed Nanotechnol 4 (2008) 99–132.

[5] Z-ZJ Lim, J-EJ Li, C-T Ng, L-YL Yung, B-H Bay, Gold nanoparticles in cancer therapy, Acta Pharmacol Sin 32 (2011) 983–990.

[6] M.R. Papasani, G. Wang, R.A. Hill, Gold nanoparticles: the importance of physiological principles to devise strategies for targeted drug delivery, Nanomedicine: NBM 8 (2012) 804–814.

[7] S. Deb, H.K. Patra, P. Lahiri, A.K. Dasgupta, K. Chakrabarti, U. Chaudhuri, Multistability in platelets and their response to gold nanoparticles, Nanomedicine: NBM 7 (2011) 376–384.

[8] M. Benkovicova, K. Vegso, P. Siffalovic, M. Jergel, S. Luby, E. Majkova, Preparation of gold nanoparticles for plasmonic applications, Thin Solid Films 543 (2013) 138–141

[9] Cancer.net (2017) http://www.cancer.net/navigating-cancer-care/how-cancer-treated/chemotherapy/side effects chemotherapy

[10] T. Konno, H. Maeda, K. Iwai, S. Maki, S. Tashiro, M. Uchida, Y. Miyauchi, Selective targeting of anti-cancer drug and simultaneous image enhancement in solid tumors by arterially administered lipid contrast medium, Cancer 54 (11) (1984) 2367–2374.

[11] L. Grislain, P. Couvreur, V. Lenaerts, M. Roland, D. Deprez-Decampeneere, P. Speiser, Int. J. Pharm. 15 (3) (1983) 335–345.

[12] E.J. Potchen, A.J. Elliott, B.A. Siegel, R. Studer, R.G. Evens, Pharmacokinetics and distribution of a biodegradable drug-carrier, J. Surg. Oncol. 3 (6) (1971) 593–602.

[13] V.J. Richardson, B.E. Ryman, R.F. Jewkes, K. Jeyasingh,M.N. Tattersall, E.S. Newlands, S.B. Kaye, Tissue distribution and tumour localization of 99m-technetium-labelled liposomes in cancer patients., Br. J. Cancer 40 (1) (1979) 35–43.

[14] G. Gregoriadis, D.E. Neerunjun, R. Hunt, Fate of a liposome-associated agent injected into normal and tumour-bearing rodents. Attempts to improve localization in tumour tissues, Life Sci. 21 (3) (1977) 357–369.

[15] R.S. Riley, E.S. Day, Gold nanoparticle-mediated photothermal therapy: applications and opportunities for multimodal cancer treatment, Wiley Interdiscip Rev Nanomed Nanobiotechnol. 9(4) (2017)

[16] C. Di Guglielmo, D.R. López, J. De Lapuente, J.M. Mallafre, M.B. Suàrez, Embryotoxicity of cobalt ferrite and gold nanoparticles: A first in vitro approach, Reprod Toxicol 30 (2010) 271-276.

[17] L.C. Kennedy, L.R. Bickford, N.A. Lewinski, A.J. Coughlin, Y. Hu, E.S. Day, J.L. West, R.A. Drezek, A New Era for Cancer Treatment: Gold-Nanoparticle-Mediated Thermal Therapies, Small 7 (2011) 169–183.

[18] J.R. Cole, N.A. Mirin, M.W. Knight, G.P. Goodrich, N.J. Halas, Photothermal efficiencies of nanoshells and nanorods for clinical therapeutic applications, J Phys Chem C 113 (2009) 12090–12094.

[19] N.S. Abadeer, C.J. Murphy, Recent progress in cancer thermal therapy using gold nanoparticles, J Phys Chem C 120 (2016) 4691–4716.

[20] Z. Qin, Y. Wang, J. Randrianalisoa, V. Raeesi, W.C.W. Chan, W. Lipinski, Quantitative comparison of photothermal heat generation between gold nanospheres and nanorods, Sci. Rep. 6 (2016) 29836.

[21] K. Jiang, D.A. Smith, A. Pinchuk, Size-Dependent Photothermal Conversion Efficiencies of Plasmonically Heated Gold Nanoparticles, J Phys Chem C, 117 (2013) 27073–27080.

[22] Nanospectra Biosciences Inc. Pilot study of aurolaseTMtherapy in refractory and/or recurrent tumors of the head and neck. Available at: https://clinicaltrials.gov/ct2/show/NCT00848042?term= auroshell&rank=2.

[23] Emily S Day, Linna Zhang, Patrick A Thompson, Janice A Zawaski, Caterina C Kaffes, M Waleed Gaber, Susan M Blaney & Jennifer L West, Vascular-targeted photothermal therapy of an orthotopic murine glioma model, 7, (2012), 1133-48.

[24] Nanospectra Biosciences Inc. MRI/US fusion imaging and biopsy in combination with nanoparticle directed focal therapy for ablation of prostate tissue. Available at: https://clinicaltrials.gov/ct2/show/NCT02680535?term=auroshell&rank=1

[25] Nanospectra Biosciences Inc. Efficacy study of aurolase therapy in subjects with primary and/or metastatic lung tumors, https://clinicaltrials.gov/ct2/show/NCT01679470?term=auroshell&rank=3

[26] M.Y. Lan, Y.B. Hsu, C.H. Hsu, C.Y. Ho, J.C. Lin, Induction of apoptosis by high-dose gold nanoparticles in nasopharyngeal carcinoma cells, Auris Nasus Larynx 40 (2013) 563-568.

[27] S.D. Perrault, C. Walkey, T. Jennings, H.C. Fischer, W.C.W. Chan, Mediating tumor targeting efficiency of nanoparticles through design, Nano Lett 9 (2009) 1909–1915.

[28] P.K. Jain, K.S. Lee, I.H. El-Sayed, M.A. El-Sayed, Calculated Absorption and Scattering Properties of Gold Nanoparticles of Different Size, Shape, and Composition: Applications in Biological Imaging and Biomedicine, J. Phys. Chem. B, 110 (2006) 7238–7248.

[29] X. Huang, M.A. El-Sayed, Gold nanoparticles: optical properties and implementations in cancer diagnosis and photothermal therapy, J. Adv. Res., 1 (1) (2010) 13–28.

[30] D.A. Giljohann, D.S. Seferos, W.L. Daniel, M.D. Massich, P.C. Patel, Gold nanoparticles for biology and medicine, Angew Chem Int Ed Engl 49 (2010) 3280-3294.

[31] P.K. Jain, S. Eustis, M.A. El-Sayed, Plasmon coupling in nanorod assemblies: optical absorption, discrete dipole approximation simulation, and exciton-coupling model, J. Phys. Chem. B, 110 (2006) 18243–18253.

[32] T.S. Hauck, T.L. Jennings, T. Yatsenko, J.C. Kumaradas, W.C.W. Chan, Enhancing the toxicity of cancer chemotherapeutics with gold nanorod hyperthermia, Adv. Mater. 2 (20) (2008) 3832–3838.

[33] A.R. Afrooz, S.T. Sivalapalan, C.J. Murphy, S.M. Hussain, J.J. Schlager, N.B. Saleh, Spheres vs. rods: The shape of gold nanoparticles influences aggregation and deposition behavior, Chemosphere 91 (2013) 93–98.

[34] E.C. Dreaden, L.A. Austin, M.A. Mackey, M.A. El-Sayed, Size matters: gold nanoparticles in targeted cancer drug delivery, Ther. Deliv. 3 (2012) 457–478.

[35] D.M. Webster, P. Sundaram, M.E. Byrne, Injectable nanomaterials for drug delivery: carriers, targeting moieties, and therapeutics, European J. Pharm. Biopharm. 84 (2013) 1–20.

[36] H. Chen, X. Zhang, S. Dai, Y. Ma, S. Cui, S. Achilefu, Y. Gu, Multifunctional gold nanostar conjugates for tumor imaging and combined photothermal and chemo-therapy, Theranostics 3 (2013) 633–649.

[37] H. Huang, X. Yang, Synthesis of polysaccharide-stabilized gold and silver nanoparticles: a green method, Carbohydr. Res. 339 (15) (2004) 2627-2631

[38] Regiel-Futyra, Development of Noncytotoxic Chitosan–Gold Nanocomposites as Efficient Antibacterial Materials, ACS Appl. Mater. Interfaces, 7 (2) (2015) 1087–1099

[39] H. Huang, X. Yang, Synthesis of Chitosan-Stabilized Gold Nanoparticles in the Absence/Presence of Tripolyphosphate, Biomacromolecules 5 (2004) 2340-2346

[40] S. Dey, M.C.D. Sherly, M.R. Rekha, K. Sreenivasan, Alginate stabilized gold nanoparticle as multidrug carrier: Evaluation of cellular interactions and hemolytic potential, Carbohydr. Polym. 136 (2016) 71–80

[41] S. Pandey, G.K. Goswami, K.K. Nanda, Green synthesis of polysaccharide/gold nanoparticle nanocomposite: an efficient ammonia sensor, Carbohydr Polym. 94 (2013) 229-34.

[42] P. Manivasagan, S. Bharathiraja, N.Q. Bui, B. Jang, Y.O. Oh, I.G. Lim, J. Oh, Doxorubicin-loaded fucoidan capped gold nanoparticles for drug delivery and photoacoustic imaging, Int J Biol Macromol. 91 (2016) 578-88.

[43] R. Kakkar, E.D. Sherly, K. Madgula, D.K. Devi, B. Sreedhar, Synergetic effect of sodium citrate and starch in the synthesis of silver nanoparticles, J. Appl. Polym. Sci. 126 (2012) 154–161

[44] D. Wisser, F.M. Wisser, S. Raschke, N. Klein, M. Leistner, J. Grothe, E. Brunner, S. Kaskel, Biological Chitin–MOF Composites with Hierarchical Pore Systems for Air-Filtration Applications, Angew. Chem. Int. Ed. 54 (2015) 12588-12591.

[45] U. Prabhakar, H.K. Maeda, R. Jain, EM. SevickMuraca, W. Zamboni, O.C. Farokhzad, S.T. Barry, A. Gabizon, P. Grodzinski, D.C. Blakey, Challenges and key considerations of the enhanced permeability and retention effect for nanomedicine drug delivery in oncology, Cancer Res 73 (2013) 2412–2417

[46] J.W. Nichols, Y.H. Bae, EPR: evidence and fallacy, J. Control. Release 190 (2014) 451–464.

[47] Y. Shigemasa, S. Minami, Applications of chitin and chitosan for biomaterials, Biotechnology and Genetic Engineering Reviews, 13 (1996) 383–420.

[48] M. J. Laudenslager, J. D. Schiffman, C. L. Schauer, Carboxymethyl chitosan as a matrix material for platinum, gold, and silver nanoparticles, Biomacromolecules, 9 (10) (2008) 2682–2685

[49] M. Venkatesham, D. Ayodhya, A. Madhusudhan, N. V. Babu, G. Veerabhadram, A novel green one-step synthesis of silver nanoparticles using chitosan: catalytic activity and antimicrobial studies, Appl. Nanosci.   4 (1) (2012) 113–119

[50] D.R. Bhumkar, H. M. Joshi, M. Sastry, V. B. Pokharkar, Chitosan Reduced Gold Nanoparticles as Novel Carriers for Transmucosal Delivery of Insulin, Pharm. Res.   24 (8) (2007) 1415–1426

[51] Z. Chen, Z. Wang, X. Chen, H. Xu, J. Liu, Chitosan-capped gold nanoparticles for selective and colorimetric sensing of heparin, J Nanopart Res, 15 (9) (2013)

[52] P. Schlinkert, E. Casals, M. Boyles, U. Tischler, E. Hornig, N. Tran, J. Zhao, M. Himly, M. Riediker, G. J. Oostingh, V. Puntes, A. Duschl,The oxidative potential of differently charged silver and gold nanoparticles on three human lung epithelial cell types, J Nanobiotechnology, 13 (1) (2015)

[53] D.R. Bhumkar, H. M. Joshi, M. Sastry, V. B. Pokharkar, Chitosan Reduced Gold Nanoparticles as Novel Carriers for Transmucosal Delivery of Insulin, Pharm. Res. 24 (8) (2007) 1415–1426

[54] Y. Hu, Q. Chen, Y. Ding, R. Li, X. Jiang, B. Liu, Entering and Lighting Up Nuclei Using Hollow Chitosan–Gold Hybrid Nanospheres, Adv. Mater. 21 (2009) 3639–3643

[55] R. Chen, X. Zheng, H. Qian, X. Wang, J.Wang, X. Jiang, Combined near-IR photothermal therapy and chemotherapy using gold-nanorod/chitosan hybrid nanospheres to enhance the antitumor effect, Biomater. Sci. 1 (2013) 285-293

[56] G. Zhang, X. Sun, J. Jasinski, D. Patel, A. M. Gobin, Gold/Chitosan Nanocomposites with Specific Near Infrared Absorption for Photothermal Therapy Applications, Journal of Nanomaterials 5 (2012)

[57] A. Topete, M. Alatorre Meda, E. M. Villar Alvarez, S. Carregal Romero, S. Barbosa, W. J. Parak, V. Mosquera, Polymeric Gold Nanohybrids for Combined Imaging and Cancer Therapy, Advanced healthcare materials, 3(8) (2014) 1309-1325.

[58] A. Topete, M. Alatorre-Meda, P. Iglesias, E. M. Villar-Alvarez, S. Barbosa, J. A. Costoya, P. Taboada, V. Mosquera, Fluorescent Drug-Loaded, Polymeric- Based, Branched Gold Nanoshells for Localized Multimodal Therapy and Imaging of Tumoral Cells, ACS nano, 8(3) (2014) 2725-2738.

[59] N. S. Rejinold , R. Jayakumar , Yeu-Chun Kim, Radio frequency responsive nano-biomaterials for cancer therapy, J. Control. Release. 204 (2015) 85-97

[60] N. S. Rejinold, R. G. Thomas, M. Muthiah, K. P. Chennazhi, In-Kyu Park, Y. Y. Jeong, K. Manzoor, R. Jayakumar, Radio frequency triggered curcumin delivery from thermo and pH responsive nanoparticles containing gold nanoparticles and its in vivo localization studies in an orthotopic breast tumor model, RSC Adv. 4 (2014) 39408

[61] N. S. Rejinold, R. G. Thomas, M. Muthiah, K. P. Chennazhi, In-Kyu Park, Y. Y. Jeong, K. Manzoor, R. Jayakumar, Anti-cancer, pharmacokinetics and tumor localization studies of pH-, RF- and thermo-responsive nanoparticles, Int J Biol Macromol. 74 (2015) 249-262.

[62] A. Rai, A. Prabhune, C. C. Perry, Antibiotic Mediated Synthesis of Gold Nanoparticles with Potent Antimicrobial Activity and Their Application in Antimicrobial Coatings. J. Mater. Chem. 20 (2010) 6789-6798.

[63] A. Regiel-Futyra, M. Kus-Lisk´iewicz, V. Sebastian, S. Irusta, M. Arruebo, G. Stochel, A. Kyziol, Development of Noncytotoxic Chitosan-Gold Nanocomposites as Efficient Antibacterial Materials, ACS Appl. Mater. Interfaces 7 (2) (2015) 1087–1099.

[64] J. Rhoades, S. Roller, Antimicrobial actions of degraded and native chitosan against spoilage organisms in laboratory media and foods, Appl. Environ. Microbiol. 66 (2000) 80.

[65] Y.L. Kuen, S.H. Wan, H.P. Won, Blood compatibility and biodegradability of partially N-acylated chitosan derivatives, Biomaterials 16 (1995) 1211.

[66] S. Hsua, Y. Changd, C. Tsaie, K. Fua, S. Wangf, H. Tsengd, Characterization and biocompatibility of chitosan nanocomposites, Colloids Surf B Biointerfaces. 85 (2011) 198–206.

[67] N. Chauhan, C.S.Pundir, Amperometric determination of acetylcholine—A neurotransmitter, by chitosan/gold-coated ferric oxide nanoparticles modified gold electrode, Biosens. Bioelectron. 61(2014)1–8.

[68] N. Tammama, M.A.F. Khalila, E. A. Gawada, A. Althanic, H. Zaghlould, H.M.E. Azzazya, Chitosan gold nanoparticles for detection of amplified nucleic acids isolated from sputum, Carbohydr. Polym. 164 (2017) 57-63.

[**69**] Z. Wei, J. Zhang, A. Zhang, Y. Wang, X. Cai, Electrochemical Detecting Lung Cancer-Associated Antigen Based on Graphene-Gold Nanocomposite. Molecules 22(3) (2017).

[**70**] P. Manivasagan, S. Bharathiraja, N.Q. Bui, I.G. Lim, J. Oh, Paclitaxel-loaded chitosan oligosaccharide-stabilized gold nanoparticles as novel agents for drug delivery and photoacoustic imaging of cancer cells. Int J Pharm. 511(1) (2016) 367-79.

[**71**] W. Zhang, Y. Du, M. L. Wang, On-chip highly sensitive saliva glucose sensing using multilayer films composed of single-walled carbon nanotubes, gold nanoparticles, and glucose oxidase, Sens Biosensing Res 4 (2015) 96-102

[**72**] J. Li, G. Zhang, L. Wang, A. Shen, J. Hu, Simultaneous enzymatic and SERS properties of bifunctional chitosan-modified popcorn-like Au-Ag nanoparticles for high sensitive detection of melamine in milk powder, Talanta. 140 (2015) 204-211

[73] A. M. Stephen, G. O. Philips, P. A. Williams, Food polysaccharides and their applications. New York: Marcel Dekker., (1995) 205–217.

[74] M.M. Paula, F. Petronilho, F. Vuolo, G.K. Ferreira, L. De Costa, G.P. Santos, P.S. Effting, F. Dal-Pizzol, A.G. Dal-Bó, T.E. Frizon, P.C. Silveira, R.A. Pinho, Gold nanoparticles and/or N-acetylcysteine mediate carrageenan-induced inflammation and oxidative stress in a concentration-dependent manner. J Biomed Mater Res A. 103(10) (2015) 3323-30.

[75] A.M. Salgueiro, A.L. Daniel-da-Silva, S. Fateixa, T. Trindade. κ-Carrageenan hydrogel nanocomposites with release behavior mediated by morphological distinct Au nanofillers. Carbohydr Polym. 91(1) (2013) 100-9.

[76] C. Esmaeili, L. Y. Heng, C.P. Chiang, Z.A. Rashid, E. Safitri, R.S.P.M. Marugan, A DNA biosensor based on kappa-carrageenan-polypyrrole-gold nanoparticles composite for gender determination of Arowana fish (Scleropages formosus), Sens Actuators B Chem. 242 (2017) 616-624.

[77] A. Martinsen, G. Skjäk-Braek, O. Smidsrod, Alginate as Immobilization Material: I. Correlation between Chemical and Physical Properties of Alginate Gel Beads. Biotechnol. Bioeng. 33 (1989) 79–89.

[78] G. R. Seely, R. L. Hart, The Binding of Alkaline Earth Metal Ions to Alginate. Macromo. 7 (1974) 706–710.

[79] W. J. Zhang, C. Laue, A. Hyder, J. Schrezenmeir, Purity of Alginate Affects the Viability and Fibrotic Overgrowth of Encapsulated Porcine Islet Xenografts. Transplant Proc. 33 (2001) 3517–3519.

[80] F. Qie, A. Astolfo, M. Wickramaratna, M. Behe, M. D. M. Evans, T.C. Hughes, X. Hao and T. Tan, Self-assembled gold coating enhances X-ray imaging of alginate microcapsules, Nanoscale 7 (2015) 2480-2488

[81] A. Astolfo, F. Qie, A. Kibleur, X. Hao , R.H. Menk, F. Arfelli, L. Rigon, T.M. Hinton, M. Wickramaratna, T. Tan, T.C. Hughes, A simple way to track single gold-loaded alginate microcapsules using x-ray CT in small animal longitudinal studies, Nanomedicine 10(8) (2014)1821-8.

[82] B. Chico, C. Camacho, M. Pérez, M.A. Longo, M.A. Sanromán, J. M. Pingarrón, R. Villalonga, Polyelectrostatic immobilization of gold nanoparticles-modified peroxidase on alginate-coated gold electrode for mediatorless biosensor construction, J. Electroanal. Chem 629 (2009) 126–132

[83] F. Lim, A.M. Sun, Microencapsulated islets as bioartificial endocrine pancreas. Science 210 (1980) 908-909

[84] A. Bule´on, P. Colonna, V. Planchot, S. Ball, Starch granules: structure and biosynthesis, Int. J. Biol. Macromol. 23 (1998) 85– 112.

[85] M. Reches, E. Gazit, Casting Metal Nanowires Within Discrete Self-Assembled Peptide Nanotubes, Science 300 (2003) 625.

[86] P, Pienpinijtham, X.X. Han, S. Ekgasit, Y. Ozak, Highly Sensitive and Selective Determination of Iodide and Thiocyanate Concentrations Using Surface-Enhanced Raman Scattering of Starch-Reduced Gold Nanoparticles Anal. Chem. 83 (2011) 3655–3662

[87] C. Engelbrekt, K. H. Sørensen, J. Zhang, A.C. Welinder, P. S. Jensen, J. Ulstrup, Green synthesis of gold nanoparticles with starch–glucose and application in bioelectrochemistry. J. Mater. Chem., 2009, 19, 7839–784

[88] S.Vantasin, P. Pienpinijtham, K. Wongravee, C. Thammacharoen, S. Ekgasit, Naked eye colorimetric quantification of protein content in milk using starch-stabilized gold nanoparticles, Sens Actuators B 177 (2013) 131– 137.

[89] T.K. Sarma, A. Chattopadhyay, Starch-mediated shape-selective synthesis of Au nanoparticles with tunable longitudinal plasmon resonance. Langmuir 20(9) (2004) 3520-4.

[90] Z. Shervani, Y. Yamamoto, Carbohydrate-directed synthesis of silver and gold nanoparticles: effect of the structure of carbohydrates and reducing agents on the size and morphology of the composites. Carbohydr Res. 346(5) (2011) 651-8.

[91] B. Duan, F. Liu, M. He, L. Zhang, Ag-Fe3O4 nanocomposites@chitin microspheres constructed by in situ one-pot synthesis for rapid hydrogenation catalysis, Green. Chem. 16 (2014) 2835-2845.

[92] E. Kim, Y. Xiong, Y. Cheng, H.-C. Wu, Y. Liu, B.H. Morrow, H. Ben-Yoav, R. Ghodssi, G.W. Rubloff, J. Shen, Chitosan to connect biology to electronics: Fabricating the bio-device interface and communicating across this interface, Polymers 7 (2014) 1-46

[93] H. Tang, C. Chang, L. Zhang, Efficient adsorption of Hg2+ ions on chitin/cellulose composite membranes prepared via environmentally friendly pathway, Chem. Eng. J. 173 (2011) 689-697.

[94] X. Li, C. Zhang, R. Zhao, X. Lu, X. Xu, X. Jia, C. Wang, L. Li, Efficient adsorption of gold ions from aqueous systems with thioamide-group chelating nanofiber membranes, Chem. Eng. J. 229 (2013) 420-428.

[95] Z. Liu, M. Li, L. Turyanska, O. Makarovsky, A. Patanè, W. Wu, S. Mann, Self-Assembly of Electrically Conducting Biopolymer Thin Films by Cellulose Regeneration in Gold Nanoparticle Aqueous Dispersions, Chem. Mater. 22 (2010) 2675-2680.

[96] X. Li, C. Zhang, R. Zhao, X. Lu, X. Xu, X. Jia, C. Wang, L. Li, Efficient adsorption of gold ions from aqueous systems with thioamide-group chelating nanofiber membranes, Chem. Eng. J. 229 (2013) 420-428.

[97] Y. Huang, Y. Fang, L. Chen, A. Lu, L. Zhang, One-step Synthesis of Size-Tunable Gold Nanoparticles Immobilized on Chitin Nanofibrils via Green Pathway and Their Potential Applications, Chem. Eng. Jour. 315 (2017) 573-582

[98] N. S. Rejinold, R. Ranjusha, A. Balakrishnan, N. Mohammed, R. Jayakumar, Gold–chitin–manganese dioxide ternary composite nanogels for radio frequency assisted cancer therapy, RSC Adv. 4 (2014) 5819-5825

[99] H. Yano, J. Sugiyama, A.N. Nakagaito, M. Nogi, T. Matsuura, M. Hikita, K. Handa, Optically Transparent Composites Reinforced with Networks of Bacterial Nanofibers, Adv. Mater. 17 (2005) 153–155

[100] C.B. Purves, Cellulose and cellulose derivatives: Part 1, in: Emil Ott, Harold M. Spurlin. (Eds.). Wiley-Interscience, New York, 1954, pp54.

[101] R. H. Marchessault, P. R. Sundararajan, In Cellulose, in the Polysaccharides. New York: Academic Press, (1983) 11

[102] J.D. Fontana, A.M. Desouza, C.K. Fontana, I.L. Torriani, J.C. Moreschi, B.J. Gallotti,S.J. Desouza, G.P. Narcisco, J.A. Bichara, L.F.X. Farah, Acetobacter cellulose pellicle as a temporary skin substitute, Appl. Biochem. Biotechnol. 24(1) (1990) 253–264.

[103] E.J. Vandamme, S. De Baets, A. Vanbaelen, K. Joris, P. De Wulf, Improved production of bacterial cellulose and its application potential, Polym. Degrad. Stab. 59 (1998) 93–99.

[104] Y. Hu, C. Wen, L. Song, N. Zhao, F.J. Xu, Multifunctional hetero-nanostructures of hydroxyl-rich polycation wrapped cellulose-gold hybrids for combined cancer therapy. J Control Release. 255 (2017) 154-163.

[105] W Wang,T.J. Zhang, D.W. Zhang, H.Y. Li, Y. Ma. Li-MinQi, Y. Zhou, X. Zhang,Amperometric hydrogen peroxide biosensor based on the immobilization of heme proteins on gold nanoparticles–bacteria cellulose nanofibers nanocomposite, Talanta 84 (1) (2015) 71-77

[106] W.K. Czaja, D.J. Young, M. Kawecki, R.M. Brown, The future prospects of microbial cellulose in biomedical applications, Biomacromolecules 8 (2007) 1–12.

[107] D. G. Wallace, J. Rosenblatt, Role of Tissue Engineered Collagen Based Tridimensional Implant on the Healing Response of the Experimentally Induced Large Achilles Tendon Defect Model in Rabbits: A Long Term Study with High Clinical Relevance. Adv. Drug Delivery Rev. 55 (2003) 1631-1649.

[108] Y. Wang, T. Azaïs, M. Robin, A. Valle´e, C. Catania, P. Legriel, G. Pehau-Arnaudet, F. Babonneau, M. M. Giraud-Guille, N. Nassif, The Predominant Role of Collagen in the Nucleation, Growth, Structure and Orientation of Bone Apatite. Nat. Mater. 11 (2012) 724- 733.

[109] K. Tao, J. Q. Wang, Y. P. Li, D. H. Xia,. H. H. Shan, H. Xu, J. R. Lu, Short Peptide-Directed Synthesis of One-dimensional Platinum Nanostructures with Controllable Morphologies. Sci. Rep. 3 (2013) 2565.

[110] L. Castaneda, J. Valle, N. Yang, S. Pluskat, K. Slowinska, Collagen Cross-Linking with Au Nanoparticles. Biomacromolecules 9 (2008) 3383-3388.

[111] M. L. Huggins, The Structure of Collagen. J. Am. Chem. Soc. 76 (1954) 4045-4046.

[112] B.K. Boekema, M. Vlig, D.L. Olde, Effect of pore size and cross-linking of a novel collagen-elastin dermal substitute on wound healing. J Mater Sci Mater Med 25 (2014) 423–433.

[113] S.A. Grant, C.S. Spradling, D.N. Grant, Assessment of the biocompatibility and stability of a gld nanoparticle collagen bioscaffold. J Biomed Mater Res Part A 102 (2014) 332–339.

[114] O. Akturk, K. Kismet, A.C. Yasti, S. Kuru, M.E. Duymus, F. Kaya, M. Caydere, S. Hucumenoglu, D. Keskin Collagen/gold nanoparticles nanocomposites: A potential skin wound healing biomaterial, Journal of Biomaterials Applications (2016) 1-19

[115] N. Fatin-Rouge, A. Milon, J. Buffle, R.R. Goulet, A. Tessier, Diffusion and Partitioning of Solutes in Agarose Hydrogels: The Relative Influence of Electrostatic and Specific Interactions, J. Phys. Chem. B 107 (2003) 12126–12137

[116] S. Kondaveeti, K. Prasad, A.K. Siddhanta, Functional modification of agarose: A facile synthesis of a fluorescent agarose-tryptophan based hydrogel, Carbohydr. Polym. 97 (2013) 165–171

[117] H.H. Jeong, J.H. Lee, Y.M. Noh, Y.G. Kim, C.S. Lee, Generation of uniform agarose microwells for cell patterning by micromolding in capillaries, Macromol. Res. 21 (2013) 534–540

[118] V. Kattumuri, M. Chandrasekhar, S. Guha, Agarose-stabilized gold nanoparticles for surface-enhanced Raman spectroscopic detection of DNA nucleosides, Appl. Phys. Lett. 88 (15) (2006) 153114.

[119] G. L. Liu and L. P. Lee, Nanowell surface enhanced Raman scattering arrays fabricated by soft-lithography for label-free biomolecular detections in integrated microfluidics. Appl. Phys. Lett. 87 (2005) 074101.

[120] X. Ma , Y. Xia , L. Ni , L. Song , Z. Wang, Preparation of gold nanoparticles–agarose gel composite and its application in SERS detection, Spectrochim Acta A Mol Biomol Spectrosc. 121 (2014) 657-661

[121] S.A. Baeurle, M.G. Kiselev, E.S. Makarova, E.A. Nogovitsin, . Effect of the counterion behavior on the shear-compressive properties of chondroitin sulfate solutions, Polymer 50 (7) (2009) 1805–1813.

[122] K.M. Jordan, N.K. Arden, EULAR Recommendations 2003: an evidence based approach to the management of knee osteoarthritis: Report of a Task Force of the Standing Committee for International Clinical Studies Including Therapeutic Trials (ESCISIT), Ann Rheum Dis. 62 (12) (2003) 1145–1155.

[123] D.O. Clegg, D.J. Reda, C.L. Harris, M.A. Klein, J.R. O'Dell, M.M. Hooper, J.D. Bradley, C.O. Bingham, M.H. Weisman, C.G. Jackson, N.E. Lane, J.J. Cush, L.W. Moreland, H.R. Schumacher, C.V. Oddis, F. Wolfe, J.A. Molitor, D.E. Yocum, T.J..Schnitzer, D.E. Furst, A.D. Sawitzke, H. Shi, K.D. Brandt, R.W. Moskowitz, H.J. Williams, Glucosamine, chondroitin sulfate, and the two in combination for painful knee osteoarthritis, New England Journal of Medicine 354 (8) 795–808.

[124] Y. Liu, H. Li, B. Guo, L. Wei, B. Chen , Y. Zhang, Gold nanoclusters as switch-off fluorescent probe for detection of uric acid based on the inner filter effect of hydrogen peroxide-mediated enlargement of gold nanoparticles, Biosens Bioelectron. 91 (2017) 734-740.

[125] D. Gurav , O.P. Varghese , O.A. Hamad , B. Nilsson , J. Hilborn , O.P. Oommen, Chondroitin Sulfate Coated Gold Nanoparticles: A New Strategy to Resolve Multidrug Resistance and Thromboinflammation, Chem Commun 52 (2016) 966-969.

[126] Y. Ma , M. Wei , X. Zhang , T. Zhao , X. Liu , G. Zhou, Spectral study of interaction between chondroitin sulfate and nanoparticles and its application in quantitative analysis, Spectrochim Acta A Mol Biomol Spectrosc, 153 (2016) 445-50.

[127] P. Dwivedi, V. Nayak, M. Kowshik, Role of gold nanoparticles as drug delivery vehicles for chondroitin sulfate in the treatment of osteoarthritis, Biotechnol Prog. 31 (2015) 1416-22.

[128] H.J. Cho , J. Oh , M.K. Choo , J.I. Ha , Y. Park , H.J. Maeng, Chondroitin sulfate-capped gold nanoparticles for the oral delivery of insulin, Int J Biol Macromol. 63 (2014) 15-20.

[129] H.J. Noh, H.S. Kim, S. Cho, Y. Park, Melamine nanosensing with chondroitin sulfate-reduced gold nanoparticles, J Nanosci Nanotechnol. 13 (2013) 8229-38.

[130] M. Kalita , S. Balivada , V.P. Swarup, C. Mencio , K. Raman , U.R. Desai, D. Troyer, B. Kuberan, A nanosensor for ultrasensitive detection of oversulfated chondroitin sulfate contaminant in heparin., J Am Chem Soc. 136 (2014) 554-7.

[131] K.B. Djagnya, Z. Wang, S. Xu, Gelatin: A Valuable Protein for Food and Pharmaceutical Industries: Review, Critical Reviews in Food Science and Nutrition. Taylor and Francis Online. 41 (6) (2010) 481–492.

[132] S. Suarasan, T. Simon, S. Boca, C. Tomuleasa, S. Astilean, Gelatin-coated Gold Nanoparticles as Carriers of FLT3 Inhibitors for Acute Myeloid Leukemia Treatment, Chem Biol Drug Des. 87 (2016) 927-35.

[133] A.M. Tutor, M.J.D. Meyer, S. Anne, Important Determinants for Fucoidan Bioactivity: A Critical Review of Structure-Function Relations and Extraction Methods for Fucose-Containing Sulfated Polysaccharides from Brown Seaweeds, Mar. Drugs. 9(10) (2011) 2106-2130.

[134] F. Atashrazm, R.M. Lowenthal, G.M. Woods, A.F. Holloway, J.L. Dickinson, Fucoidan and Cancer: A Multifunctional Molecule with Anti-Tumor Potential, Mar Drugs. 13(4) (2015) 2327–2346.

[135] J.Y. Kwak, Fucoidan as a Marine Anticancer Agent in Preclinical Development, Mar. Drugs 12(2) (2014) 851–870.

[136] M. Tengdelius, D. Gurav, P. Konradsson, P. Påhlsson, M. Griffith, O.P. Oommen, Synthesis and anticancer properties of fucoidan-mimetic glycopolymer coated gold nanoparticles, Chem Commun (Camb). 51 (2015) 8532-5.

[137] Z. Lutfi, A. Nawab, F. Alam, A. Hasnain, S.Z. Haider, Influence of xanthan, guar, CMC and gum acacia on functional properties of water chestnut (*Trapa bispinosa*) starch, Int J Biol Macromol. 103 (2017) 220-225.

 [138] W.Y. Chen, G. Abatangelo, Functions of hyaluronan in wound repair, Wound Repair Regen. 7 (2) (1999) 79–89.

[139] B.P. Toole, Hyaluronan-CD44 Interactions in Cancer: Paradoxes and Possibilities Clin. Cancer Res. 15 (2009) 7462–7468.

[140] S.P. Singh, M. Sharma, P.K. Gupta, Cytotoxicity of curcumin silica nanoparticle complexes conjugated with hyaluronic acid on colon cancer cells, Int J Biol Macromol. 74 (2015) 162–170.

[141] M.S. Karbownik, J.Z. Nowak, Hyaluronan: Towards novel anti-cancer therapeutics, Pharmacol. Rep. 65 (2013) 1056–1074.

[142] P. Jin, Z. Kang, N. Zhang, G. Du, J. Chen, High-yield novel leech hyaluronidase to expedite the preparation of specific hyaluronan oligomers, Sci. Rep. 4 (4471) (2014) 1–8.

[143] B.P. Toole, S. Ghatak, S. Misra, Hyaluronan oligosaccharides as a potential anticancer therapeutic, Curr. Pharm. Biotechnol. 9 (2008) 249–252.

[144] B.P. Toole, M.G. Slomiany, Hyaluronan, CD44 and Emmprin: partners in cancer cell chemoresistance, Drug Resist. Updat. 11 (2008) 110–121.

[145] H. Hosseinzadeh, F. Atyabi, B.S. Varnamkhasti, R. Hosseinzadeh, S.N. Ostad, M.H. Ghahremani, R. Dinarvand, SN38 conjugated hyaluronic acid gold nanoparticles as a novel system against metastatic colon cancer cells, Int J Pharm, 526 (2017) 339-352.

[146] B. Li, P. Zhang, J. Du, X. Zhao, Y. Wang, Intracellular fluorescent light-up bioprobes with different morphology for image-guided photothermal cancer therapy, Colloids Surf B Biointerfaces. 154 (2017) 133-141.

[147] C.S. Kumar, M.D. Raja, D.S. Sundar, M. G. Antoniraj, K. Ruckmani, Hyaluronic acid co-functionalized gold nanoparticle complex for the targeted delivery of metformin in the treatment of liver cancer (HepG2 cells) Carbohydr Polym. 128 (2015) 63-74.

[148] L. Zhao, T.H. Kim, H.W. Kim, J.C. Ahn, S.Y. Kim, Surface-enhanced Raman scattering (SERS)-active gold nanochains for multiplex detection and photodynamic therapy of cancer, Acta Biomater. 20 (2015) 155-64.

[149] C.M. Lin, W.C. Kao, C.A. Yeh, H.J. Chen, S.Z. Lin, H.H. Hsieh, W.S. Sun, C.H. Chang, H.S. Hung, Hyaluronic acid-fabricated nanogold delivery of the inhibitor of apoptosis protein-2 siRNAs inhibits benzo[a]pyrene-induced oncogenic properties of lung cancer A549 cells, Nanotechnology. 26 (2015) 105101.

[150] J. Li, Y. Hu, J. Yang, P. Wei, W. Sun, M. Shen, G. Zhang, X. Shi, Hyaluronic acid-modified Fe3O4@Au core/shell nanostars for multimodal imaging and photothermal therapy of tumors, Biomaterials. 38 (2015) 10-21.

[151] Y. Song , Z. Wang , L. Li , W. Shi , X. Li , H. Ma, Gold nanoparticles functionalized with cresyl violet and porphyrin via hyaluronic acid for targeted cell imaging and phototherapy, Chem Commun (Camb). 50 (2014) 15696-8.

[152] N. Li , Y. Chen , Y.M. Zhang , Y. Yang , Y. Su , J.T. Chen , Y. Liu, Polysaccharide-gold nanocluster supramolecular conjugates as a versatile platform for the targeted delivery of anticancer drugs, Sci Rep. 4 (2014) 41-64.

[153] M. Stéphane, Joly, J. Pierre, C. Blandine, Elysée, J. Ghermani, N. Eddine; M. Alain , Synthesis and inclusion ability of a bis-β-cyclodextrin pseudo-cryptand towards Busulfan anticancer agent, Tetrahedron. 63 (7) (2007) 1706.

[154] T.R. Thatiparti, A.J. Shoffstall, H.A.Von Recum, Cyclodextrin-based device coatings for affinity-based release of antibiotics, Biomaterials 31 (8) (2010) 2335–47.

[155] B. Gordon, S.L. J, T.M. Yee, Simultaneous liquid chromatographic analysis of catecholamines and 4-hydroxy-3-methoxyphenylethylene glycol in human plasma: comparison of amperometric and coulometric detection, International Journal of Pharmaceutics. 179 (1) (1999) 65–71.

[156] Y. Hu , C. Wen , L. Song , N. Zhao , F.J. Xu, Multifunctional hetero-nanostructures of hydroxyl-rich polycation wrapped cellulose-gold hybrids for combined cancer therapy, J Control Release. 255 (2017) 154-163.

[157] D. Lee , W.K. Ko , D.S. Hwang, D.N. Heo, S.J. Lee, M. Heo, K.S. Lee, J.Y. Ahn, J. Jo, Kwon IK, Use of Baicalin-Conjugated Gold Nanoparticles for Apoptotic Induction of Breast Cancer Cells, Nanoscale Res Lett. 11 (2016) 381.

[158] W.H. Chen, Q. Lei, G.F. Luo, H.Z. Jia, S. Hong, Y.X. Liu, Y.J. Cheng, X.Z. Zhang, Rational Design of Multifunctional Gold Nanoparticles via Host-Guest Interaction for Cancer-Targeted Therapy, ACS Appl Mater Interfaces. 7 (2015) 17171-80.

[159] F. Bakar, M.G. Caglayan, F. Onur, S. Nebioglu, I.M. Palabiyik, Gold nanoparticle-lignan complexes inhibited MCF-7 cell proliferation in vitro: a novel conjugation for cancer therapy, Anticancer Agents Med Chem. 15 (2015) 336-44.

[160] A.J. Mieszawska, Y. Kim, A. Gianella, I. van Rooy, B. Priem, M.P. Labarre, C. Ozcan, D.P. Cormode, A. Petrov, R. Langer, O.C. Farokhzad, Z.A. Fayad, W.J. Mulder, Synthesis of polymer-lipid nanoparticles for image-guided delivery of dual modality therapy, Bioconjug Chem. 24 (2013) 1429-34.

[161] D.N. Heo, D.H. Yang, H.J. Moon, J.B. Lee, M.S. Bae, S.C. Lee, W.J. Lee, I.C. Sun, I.K. Kwon, Gold nanoparticles surface-functionalized with paclitaxel drug and biotin receptor as theranostic agents for cancer therapy, Biomaterials. 33 (2012) 856-66.

[162] A. Anitha, V.G. Deepagan, V.V. Divya Rani, D. Menon, S.V. Nair, R. Jayakumar, Preparation, characterization, in vitro drug release and biological studies of curcumin loaded dextran sulphate–chitosan nanoparticles, Carbohydr Polym, 84 (3) (2011) 1158–1164.

[163] C.Y. Falcoa, P. Falkmanb, J. Risboa, M. Cárdenas, B. Medronhoc, Chitosan-dextran sulfate hydrogels as a potential carrier for probiotics, Carbohydr Polym 172 (2017) 175–183

[164] B. Saksono, B.E. Dewi, L. Nainggolan, Y. Suda, A Highly Sensitive Diagnostic System for Detecting Dengue Viruses Using the Interaction between a Sulfated Sugar Chain and a Virion, PLoS One. 10 (2015) **e0123981.**

[165] A. Charrier, N. Candoni, N. Liachenko, F. Thibaudau, 2D aggregation and selective desorption of nanoparticle probes: a new method to probe DNA mismatches and damages, Biosens Bioelectron. 22 (2007) 1881-6.

[166] L. Li, M. Nurunnabi, M. Nafiujjaman, Y. Y. Jeong, Y. k. Lee, K. M. Huh, A photosensitizer-conjugated magnetic iron oxide/ gold hybrid nanoparticle as an activatable platform for photodynamic cancer therapy, Journal of Materials Chemistry B 2 (2014) 2929-2937.

[167] L. Li, M. Nurunnabi, M. Nafiujjaman, Y. k. Lee, K. M. Huh, GSH-mediated photoactivity of pheophorbide a-conjugated 2 heparin/gold nanoparticle for photodynamic therapy, 171 (2) (2013) 241-250.

[168] S. H. Kang, M. Nafiujjaman, M. Nurunnabi, L. Li, H. A. Khan, K. J. Cho, K. M. Huh, Y. k. Lee, Hybrid Photoactive Nanomaterial Composed of Gold Nanoparticles, Pheophorbide-A and Hyaluronic Acid as a Targeted Bimodal Phototherapy, Macromolecular Research 23 (2015) 474-484.

[169] Pilot Study of AuroLase(tm) Therapy in Refractory and/or Recurrent Tumors of the Head and Neck, https://clinicaltrials.gov/ct2/show/NCT00848042 (accessed on 20 September 2017)

[170] A Phase I/II Study of ODX (Osteodex) in Metastatic Castration Resistant Prostate Cancer (CRPC), https://clinicaltrials.gov/ct2/show/NCT01595087 (accessed on 20 September 2017)

[171] CRLX101 in Combination With Bevacizumab for Recurrent Ovarian/Tubal/Peritoneal Cancer, https://clinicaltrials.gov/ct2/show/NCT01652079 (accessed on 20 September 2017)

Figures
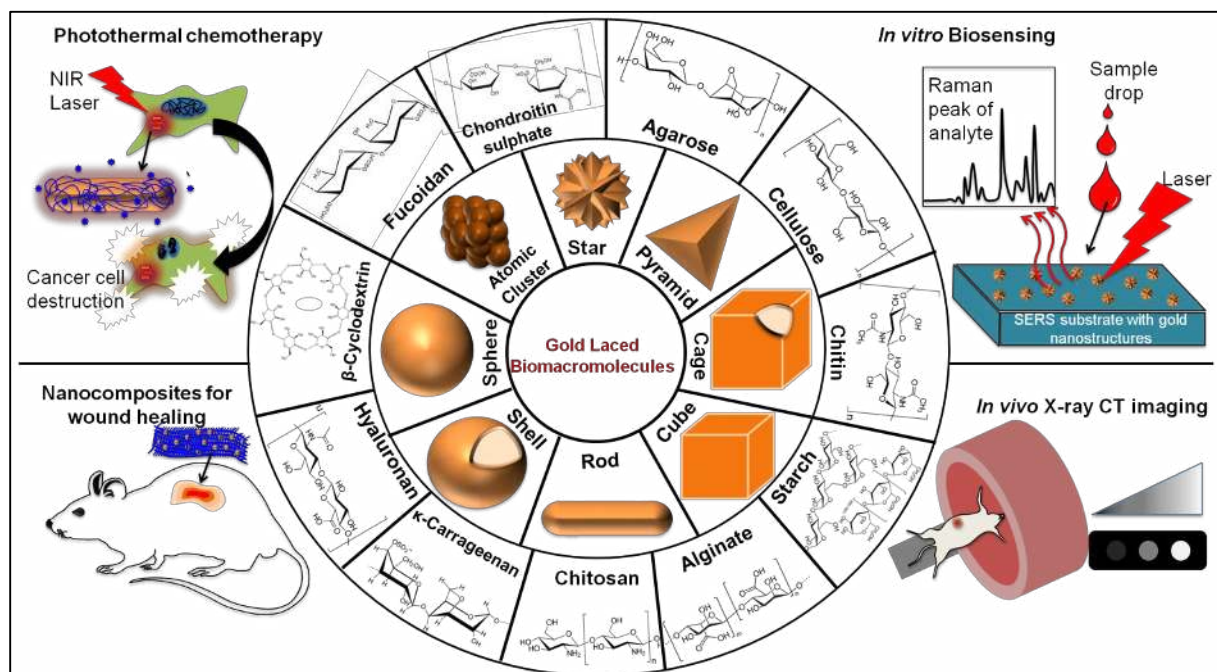
Figure 1: Gold nanostructures combined with functional biomacromolecules for therapeutic and diagnostic applications
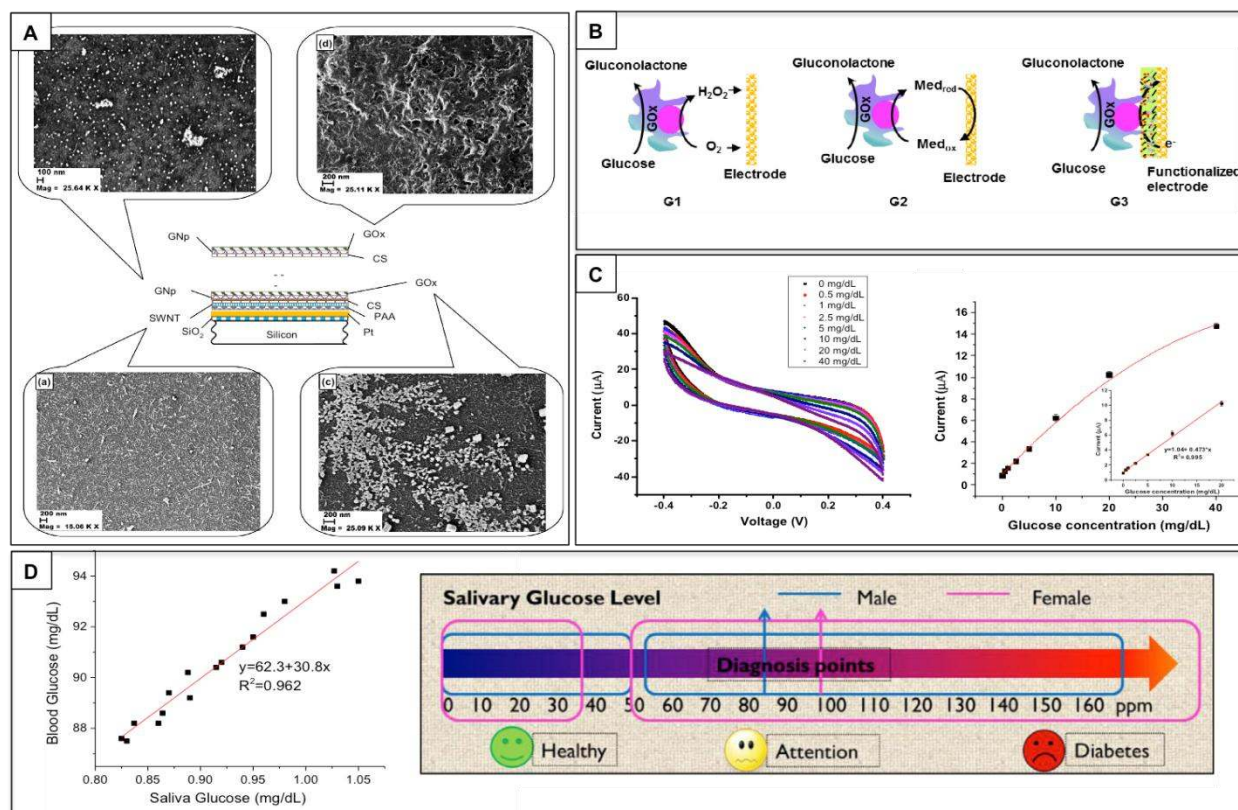
Fig. 2: (A) Cross-section of the functional layers on the sensor electrode and SEM images of one layer of SWNT (top left corner); one layer of SWNT/GNp (top right corner); PAA/SWNT/CS/GNp/GOx film (bottom left corner); PAA/SWNT/(CS/GNp/GOx)$_3$ (bottom right corner);) film on the sensor electrode surface. **(B)** A general scheme depicting the three enzymatic glucose detection mechanisms, presented as the first (G1), second (G2), and third (G3) generation glucose sensors. **(C)** Glucose sensing using the on-chip electrochemical sensing system S2D2 by cyclic voltammetry of Pt electrode modified with PAA/SWNT/ (CS/GNp/GOx)$_3$ layers obtained in 0–40 mg/dL glucose solutions with the voltage between WE and RE ranges from -0.4 V to 0.4 V at a scan rate of 50 mV/s; steady-state calibration curve of the PAA/SWNT/(CS/GNp/GOx)3 functionalized Pt electrode at applied potential 0.2 V with linear detection range shown in the inset. Error bars = ± standard deviation and n = 3. **(D)** Correlation between blood glucose and saliva glucose of a healthy subject at fasting state; summarized saliva glucose levels indicating individuals' health conditions from literature [56].
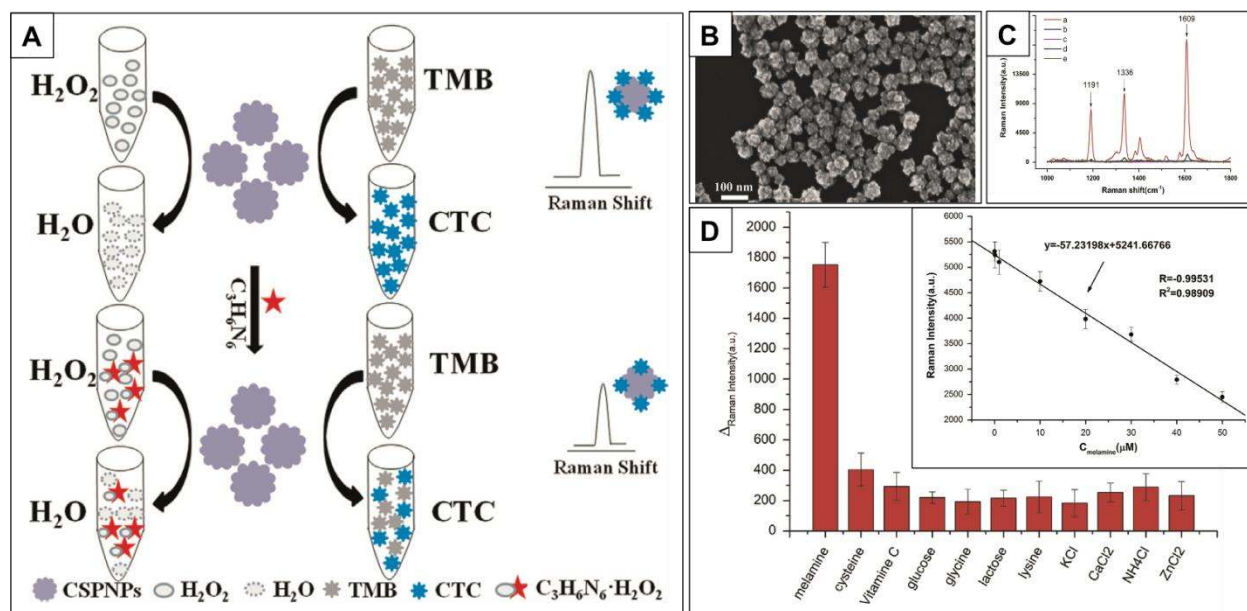
Fig. 3: (A) Design of the SERRS detection of melamine using CSPNPs. **(B)** SEM image of CSPNPs showing "nanodots" with the size of about 10nm, just like the petals of popcorns with a particle size of 80 nm. **(C)** Raman spectra of different reaction solutions **(a)** H_2O_2, TMB, CSPNPs; **(b)** TMB, CSPNPs; **(c)** H_2O_2, CSPNPs; **(d)** H_2O_2, TMB; **(e)** CSPNPs. **(D)** The selectivity of the proposed method towards melamine detection. Inset graph illustrates the linear calibration plot for melamine detection [57].
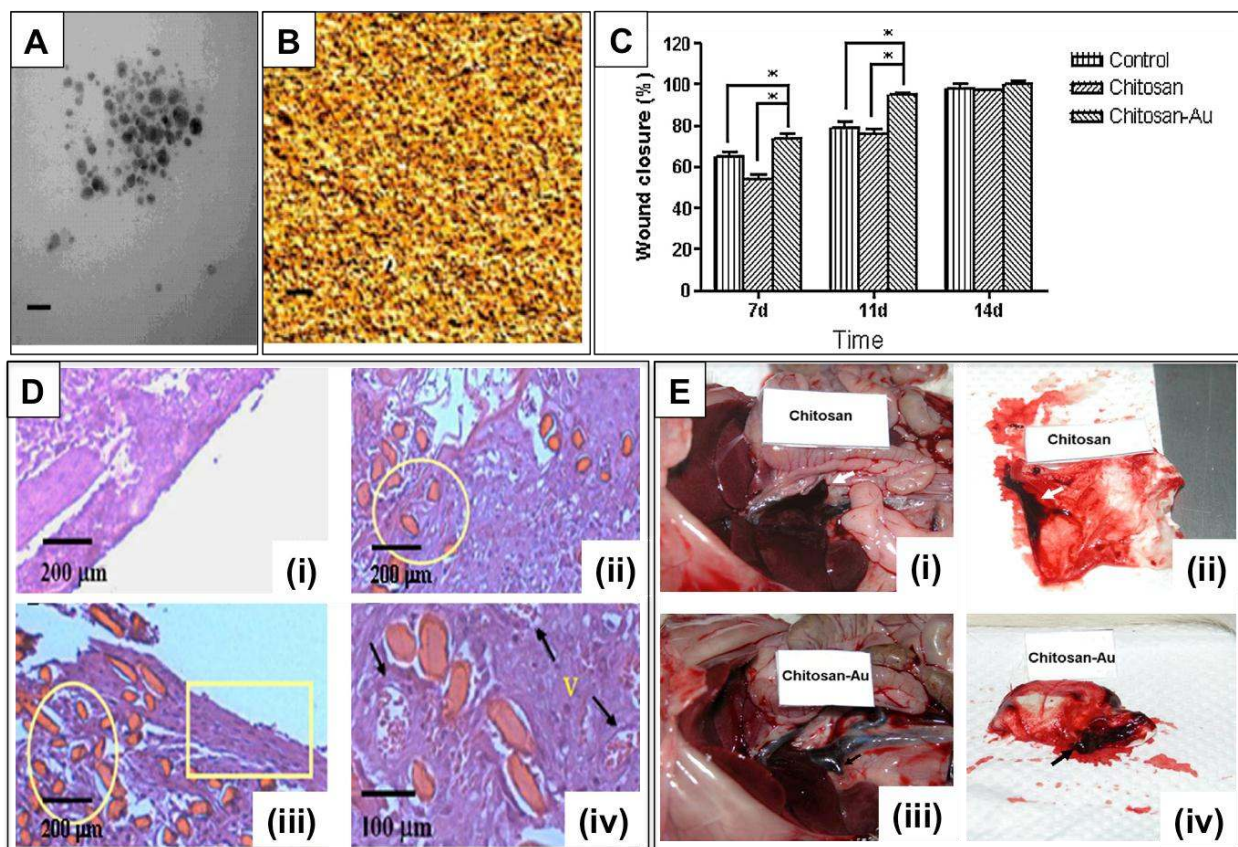
Fig. 4: **(A)** TEM image and **(B)** AFM image of chitosan-Au composite (Au content-120 ppm). **(C)** A comparison between Chitosan and Chitosan-Au for wound repair for the rat dorsal skin (for n = 5) evaluated as the wound healing ratio from different dressings (*p < 0.05). **(D)** The histology of the wound obtained at 7 days post surgery for: **(i)** control group (Tegaderm) (100×), **(ii)** chitosan group (100X), **(iii)** chitosan-Au group (100X) and **(iv)** chitosan-Au group at higher magnification (200X). **(E)** Hemostatic evaluation for chitosan: **(i)** bleeding (marked by the white arrow) from the rat hepatic portal vein and **(ii)** the appearance of dressing after removal; and that for chitosan-Au nanocomposites: **(iii)** hemostasis in the rat portal vein (blot clot marked by the black arrow) and **(iv)** the appearance of dressing after removal [70].
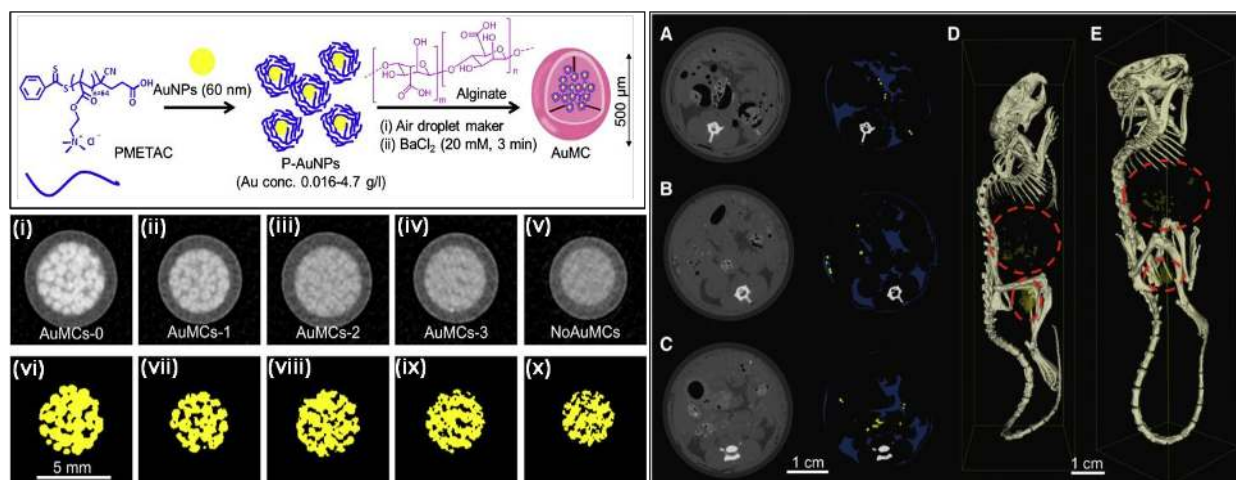
Fig. 5: Left top panel showing gold nanoparticles incorporated in alginate microcapsules (AuMCs) preparation. Left bottom panel showing MCs *in vitro* micro-CT data acquired at a low entrance dose at different AuNP concentration (i-v) and their segmentations (yellow in vi-x) Right panel showing low dose CT reconstructed single slices (54 μm thick) of the mice injected with AuMCs-0 (A), AuMCs-1 (B), and AuMCs-2 (C) at the peritoneal cavity height in gray scale and the corresponding slices with fat tissue, AuMCs, and bone segmented in blue, yellow, and white, respectively. 3D rendering of the entire mice injected with AuMCs-0 (D) and AuMCs-1 (E) acquired with the preclinical micro-CT scanner at 116 μm isotropic voxel size. The AuMCs are segmented in yellow and outlined with red dashed circles [80].
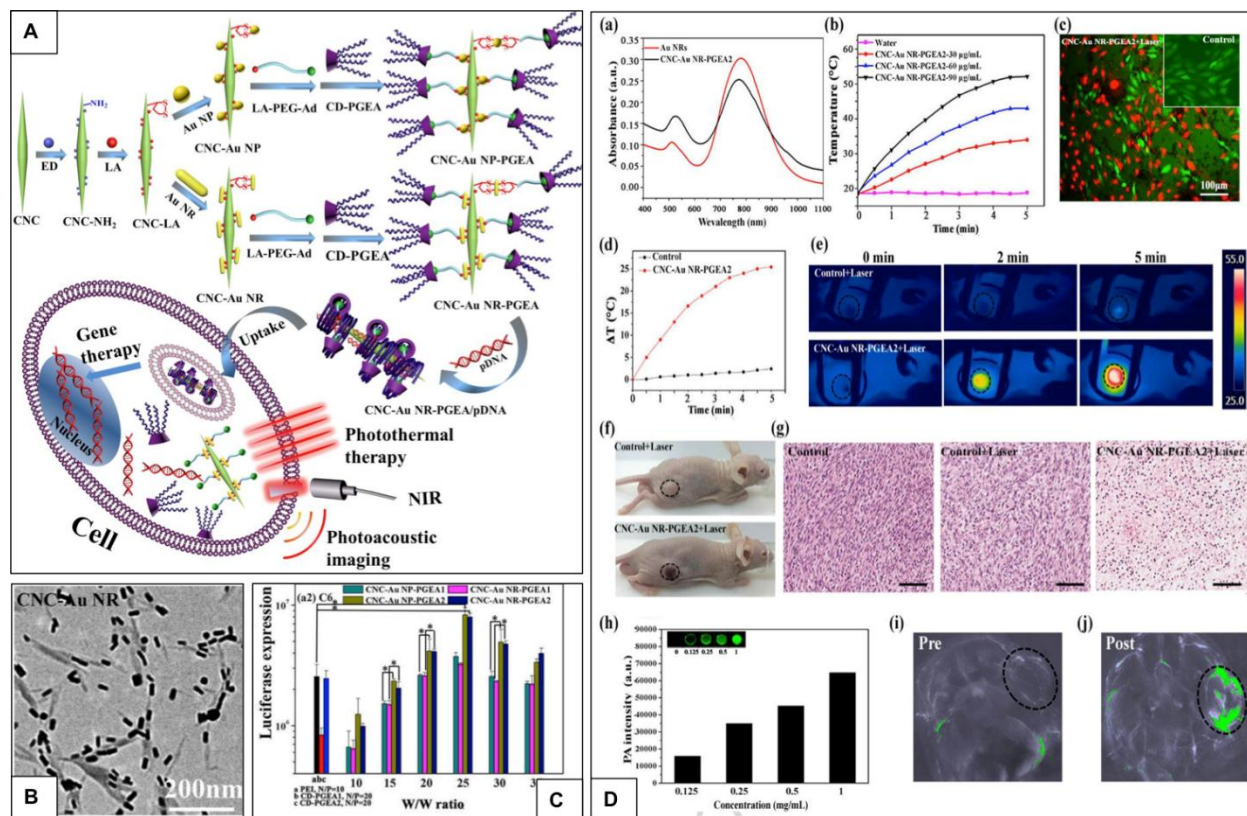
Fig. 6: (A) Synthesis of CNC-Au NP-PGEA and CNC-Au NR-PGEA **(B)** TEM images of CNC-Au NR. **(C)** In vitro gene transfection efficiencies of plasmid pEGFP-N1 encoding enhanced green fluorescent protein (EGFP). Administration of CNC-Au-PGEA/pDNA complexes at various W/W ratios compared with those of PEI (at its optimal N/P ratio of 10, black bar) and CD-PGEA (CD-PGEA1 (red bar) and CD-PGEA2 (blue bar) at their optimal N/P ratios of 20 in C6 cell lines. **(D)(a)** Vis-NIR absorption spectra of Au NR and CNC-Au NR-PGEA2. **(b)** Temperature elevation of water and CNC-Au NR-PGEA2 solutions with different concentrations (30 to 90 µg/mL) as a function of irradiation time. **(c)** Fluorescence images of C6 cells with and without CNC-Au NR-PGEA2 after irradiation at 808 nm (2 W/cm^2),The cells stained with propidium iodide (dead cells) while cells stained via fluorescein diacetate (live cells) **(d)** Temperature variation by IR thermal camera shows the temperature variation at the tumor site **(e)** Infrared thermal images recorded at the irradiation time of 0, 2 and 5 min **(f)** Images of C6 tumor-bearing mice after injection with PBS or CNC-Au NR-PGEA2 and further exposed with 808 nm laser (2 W/cm^2). **(g)** H & E stained images of dissected tumors after different treatments (scale bars: 100 µm). **(h)** PA intensity and images (inset) of CNC-Au NR-PGEA2 solutions at different concentrations. PA images of CNC-Au NR-PGEA administered mice **(i)** before and **(j)** after intratumoral injection with tumor site (being highlighted by black dotted circles) showing enhanced PA signal (green) by CNC-Au NR-PGEA2 [104].

Table-1: Summary of various gold nanoparticle (AuNP) – Biomacromolecule composites for therapy and diagnostic applications.

S. No.	Composite	Active Ingredient	Application	Reference
1.	Chitosan AuNPs	Insulin	Drug delivery	[53]
2.	Chitosan oligosaccharides AuNPs	Paclitaxel	Drug delivery and PAI	[55]
3.	Chitosan AuNPs	Poly acrylic acid/cisplatin	Drug delivery	[58]
4.	Chitosan gold nanohybrids	DOXO/SPION-PLGA	PDT and fluorescence-based imaging	[61], [62]
5.	Chitosan AuNPs	Fe_3O_4/acetylcholinesterase /cholineoxidase	Amperometric sensor	[71]
6.	Kappacarrageenan-AuNPs	Polypyrrole	Biosensor	[76]
7.	AuNPs incorporated in alginate microcapsules	-	Micro-CT tracking	[80]
8.	Alginate- AuNPs	Peroxidase	Amperometric sensor	[82]
9.	Starch- AuNPs	-	Biosensor	[88]
10.	Gold based chitin–MnO_2 ternary composite nanogels	-	magnetic hyperthermia	[98]
11.	Bacterial cellulose-AuNPs/AuNRs	-	Gene therapy and PAI	[104]

12.	AuNP-cellulose nanocomposite	Heme proteins	Amperometric sensor	[105]
13.	Collagen/AuNPs	-	Wound healing	[114]
14.	Agarose-stabilized AuNPs	-	SERS	[118], [119]
15.	AuNPs–agarose gel	-	SERS	[120]
16.	Chondroitin sulfate (CS) coated AuNPs	Insulin	Drug delivery	[128]
17.	Fucoidan capped AuNPs	Doxorubicin	Drug delivery and PAI	[42]
18.	Fucoidan-mimetic glycopolymers coated AuNPs	-	Anti-cancer	[136]
19.	Guar Gum/AuNPs nanocomposite	-	SPR based biosensor	[41]
20.	Thiolated-hyaluronic acid coated gold nanorods and nanospheres	Nile Blue	Imaging and Photothermal therapy	[146]
21.	HA coated AuNPs	IAP-2-specific small-interfering RNA	Anti-cancer	[149]
22.	HA functionalized AuNPs	Cresyl violet and porphyrin	Phototherapy and fluorescence imaging	[151]
23.	AuNP-Cyclodextrin	Peptide AD-PEG8-	Anti-cancer	[158]

		GRGDS	Therapy	
24.	β-cyclodextrin modified AuNPs	Lignans (lariciresinol, pinoresinol and secoisolariciresinol)	Imaging and drug delivery	[159]
25.	β-cyclodextrin functionalized AuNPs	Rhodamine B	Cancer theranostics	[161]
26.	Dextran sulfate-AuNPs	Sulfated sugar chain	Diagnosis of Dengue virus	[164]